

This is an Open Access document downloaded from ORCA, Cardiff University's institutional repository:<https://orca.cardiff.ac.uk/id/eprint/139917/>

This is the author's version of a work that was submitted to / accepted for publication.

Citation for final published version:

Jing, Rui, Li, Yubing, Wang, Meng, Chachuat, Benoit, Lin, Jianyi and Guo, Miao 2021. Coupling biogeochemical simulation and mathematical optimisation towards eco-industrial energy systems design. *Applied Energy* 290 , 116773. 10.1016/j.apenergy.2021.116773

Publishers page: <http://dx.doi.org/10.1016/j.apenergy.2021.116773>

Please note:

Changes made as a result of publishing processes such as copy-editing, formatting and page numbers may not be reflected in this version. For the definitive version of this publication, please refer to the published source. You are advised to consult the publisher's version if you wish to cite this paper.

This version is being made available in accordance with publisher policies. See <http://orca.cf.ac.uk/policies.html> for usage policies. Copyright and moral rights for publications made available in ORCA are retained by the copyright holders.



# Coupling biogeochemical simulation and mathematical optimisation towards eco-industrial energy systems design

Rui Jing <sup>a</sup>, Yubing Li <sup>b</sup>, Meng Wang <sup>c</sup>, Benoit Chachuat <sup>b</sup>, Jianyi Lin <sup>a\*</sup> ✉, Miao Guo <sup>d\*</sup> ✉

*a Key Lab of Urban Environment and Health, Institute of Urban Environment, Chinese Academy of Sciences,  
Xiamen, China*

*b Department of Chemical Engineering, Imperial College London, South Kensington Campus, SW7 2AZ, UK*

*c School of Mechanical Engineering, Tongji University, Shanghai, China*

*d Department of Engineering, King's College London, Strand Campus, WC2R 2LS, UK*

## Abstract

Process industry remains one of the difficult-to-decarbonise sectors globally. To mitigate industrial greenhouse gas (GHGs) emissions, an eco-industrial energy system (e-IES) optimisation framework is proposed by coupling mathematical optimisation with clustering algorithms and first principle modelling. Within the framework, a rooftop farming database was developed using biogeochemical simulations, which models seven crop growth in response to 10 cultivation conditions. Clustering algorithm was applied to analyse energy system data, along with the rooftop farming database, to inform the optimisation model. A Mixed Integer Linear Programming optimisation model was developed to optimize system design considering the trade-off between economic and environmental objectives. The implications of rooftop design on e-IES and their interactive effects on industrial decarbonisation were addressed. A case study at an industrial park in Suzhou China reveals that rooftop farming could generate mutual benefits from both cost and GHG reduction perspectives. Planting lettuce indicates a cost-efficient solution, and planting tomato could contribute the most to GHG emission reduction. Compared to the rooftop PV and the spare rooftop, 2.4% and 5.6% cost savings, as well as 10.2% and 16.3% emission savings, could be achieved respectively by implementing rooftop farming. Overall, this study demonstrates an emerging perspective on decarbonising the industrial sector by coupling biogeochemical simulation and energy system optimisation and adopting cross-disciplinary approaches.

**Keyword:** integrated energy system; rooftop farming; rooftop agriculture; food-energy nexus; industrial sector decarbonisation; multi-objective optimisation

---

\*Corresponding author.

E-mail ✉: [jylin@iue.ac.cn](mailto:jylin@iue.ac.cn) (J.L.)     [miao.guo@kcl.ac.uk](mailto:miao.guo@kcl.ac.uk) (M.G.)

# 1 Introduction

The global decarbonisation agenda requires a significant reduction in greenhouse gas emissions (GHG) by 2050 comparing with 1990 levels. Process industry remains one of the difficult-to-decarbonise sectors accounting for roughly 1/4 of global GHG emissions in 2019 [1], which mainly arise through direct emissions from combustion in manufacturing processes and refining of petroleum products and fossil fuels [2]. At regional or national levels, carbon reduction targets and regulations have been introduced to mitigate climate change. EU committed to decrease 40% the industrial GHG emissions for the industry by 2030 compared to 1990 levels [3]. The Chinese government is very likely to accomplish its announced plans to reduce industrial CO<sub>2</sub> emission intensity by 22% from 2015 to 2020 [4].

There has been an increasing interest in how to cost-effectively decarbonise industrial processes. The multi-energy systems that synergistically integrates multiple types of energy, including fuel, steam, electricity, heating, and cooling, has been considered as a promising solution to mitigate industrial GHG emissions. Relevant research on decarbonisation by multi-energy systems, especially in the difficult-to-decarbonise process industry, has been reviewed as follows.

## 1.1 Relevant research

Recently published research has covered a wide range of multi-energy system optimisation [5], including the system optimisation with uncertainties [6]; sizing and operating co-optimisation [7]; quantifying the flexibility and contribution for local renewable consumption [8]; and robust system design under extreme events [9].

In particular, Process Systems Engineering research communities have contributed to mathematical optimisation development and applications in industrial multi-energy systems. Martin et al. [10] established a mixed-integer nonlinear programming optimisation model to design a self-sufficient algae biodiesel production system by integrating solar and wind energy. Wu et al. [11] developed a life cycle optimisation model considering economic and environmental objectives. Lee et al. [12] investigated the positive interaction between polygeneration and geothermal energy utilisation and highlighted the vital roles of the multi-scale modelling framework to achieve a sustainable industrial energy solution. Xu et al. [13] proposed an optimisation model to optimise energy supply and demand strategies of an industrial park, where climate uncertainties and energy systems efficiency and stability have been considered. Shen et al. [14] coupled performing exergy analysis and multi-objective optimisation to model a separation process in ethylene manufacturing and address the trade-

off between exergy efficiency and operational cost. Noorollahi et al. [15] investigated the introduction of electric vehicles as the energy storage for optimal design of energy systems in an industrial zone. Wu et al. [16] proposed a biomass polygeneration integrated energy system optimisation model and investigated the feasibility to various case regions, where the vital factor of the split ratios was further evaluated.

To harness data advances in sectoral-specific energy systems e.g. real-time energy demand and supply profiles, data-driven modelling approaches have been developed to couple machine learning techniques and mathematical optimisation [17]. Clustering algorithms in the industrial context have been summarised by Benabdellah et al. [18]. In their research, five categories of clustering techniques have been grouped: the partitioning-based, e.g. K-mean and hierarchical-based, algorithms have been used in temporal clustering in previous published research; whereas grid-based and density-based algorithms, e.g. OPTICS, have been widely applied in spatial clustering problems. Research efforts have also been placed on developing clustering algorithms to decompose spatial complexity to enable large-scale energy system optimisation models [19]. Voulis et al. [20] proposed a spatial-temporal informed clustering method to analyse electricity demand at different urban scales. Previous research also compared conventionally partitioning and hierarchical clustering algorithms with shape-based clustering algorithms, (e.g. k-shape and dynamic time warping barycenter averaging) in time-series decomposition e.g. to identify the representative period for energy systems optimisation [21]. Yilmaz et al. [22] proposed a k-means based method and combined with five features to determine the temporal representative domestic electrical demand profiles. In addition, Shen et al. [23] developed deterministic and robust optimisation models for large-scale industrial energy systems, where a data-driven approach underpinned by kernel support vector clustering was proposed to consider uncertainty parameters. Wang et al. [24] introduced a X-means clustering approach in energy system optimisation field, which is combined K-means with the Bayesian Information Criterion to evaluate surviving clusters, and further combined with a stochastic optimisation model. As highlighted in the recent review by Rajabi et al. [25], the development of efficient methods for clustering real-time and short-term data represents a future research direction.

## **1.2 Knowledge gap and contribution**

Despite that the previous energy systems modelling advances addressed multi-energy solutions under industrial settings considering energy-only components, e.g., wind turbine, solar PV panels, and solar thermal collectors, modelling gap emerges on the novel solutions by introducing eco-design components, i.e., rooftop agriculture, to enable cost-effective decarbonisation. Synergistic integration of eco-design of rooftop farming with energy supply-

demand strategy could potentially offer a promising decarbonisation solution to the process industry.

To fill this gap, this exploratory study, for the first time, models an eco-industrial energy system (e-IES), which is underpinned by considering multi-energy and rooftop farming simultaneously. We present a model-based design optimisation platform by coupling mathematical optimisation with clustering algorithms and first principle modelling to address open research questions on implications of rooftop design on e-IES and their interactive effects on decarbonisation. Through an e-IES case study, we demonstrate the new insights such an integrated model-based approach could generate to inform industrial park designer and policy-makers' decision-making.

The contributions of the present study are:

(1) The modelling scope is extended beyond multi-energy solutions that leads to highly cross-disciplinary research and has the potential to unlock the difficult-to-decarbonate industrial challenges cost-effectively. Synergistic optimisation of rooftop agriculture and industrial energy systems converges low-carbon and multi-sector co-development towards an eco-industry future.

(2) A new model-based framework has been proposed that integrates the mathematical optimisation and first principle modelling to optimise the whole system performances and generate new evidence on the co-benefits and interaction between rooftop farming and industrial energy system.

This paper is organised as follows. The modelling methods are described in Section 2. A case study is introduced in Section 3. Section 4 focuses on discussing results, limitations and future research directions, which is followed by a conclusion in Section 5.

## 2 Method

As demonstrated in Figure 1, the e-IES concept integrates rooftop farming with energy system design under the industrial park context. Implementing rooftop farming offers a potential solution to zero food miles, GHG reduction by photosynthetic assimilation of CO<sub>2</sub>, and thermal demand reduction by enhancing building rooftop insulations. Figure 1 shows the proposed model-based e-IES design optimisation framework including three major components. A rooftop farming database was constructed in the first component by first-principle underpinned simulation using DeNitrification-DeComposition (DNDC) [26], which models daily incremental growth and agro-ecosystem carbon nitrogen cycles in response to varying cultivation conditions. In the second component, unsupervised learning clustering

methods were adopted to analyse the energy system data. The model-based e-IES design optimisation forms the basis of the third component to optimise the cost-effective decarbonisation strategies for industrial park energy systems considering dataflows from the previous two components.

Specifically, the model-based e-IES design optimisation framework addresses conflicting e-IES design criteria from economic and decarbonisation perspectives. By solving the optimisation model, the rooftop utilisation options, the e-IES systematic configurations, the energy (i.e. cooling and heating) network connections, as well as the e-IES operational strategies, can be optimised holistically and simultaneously.

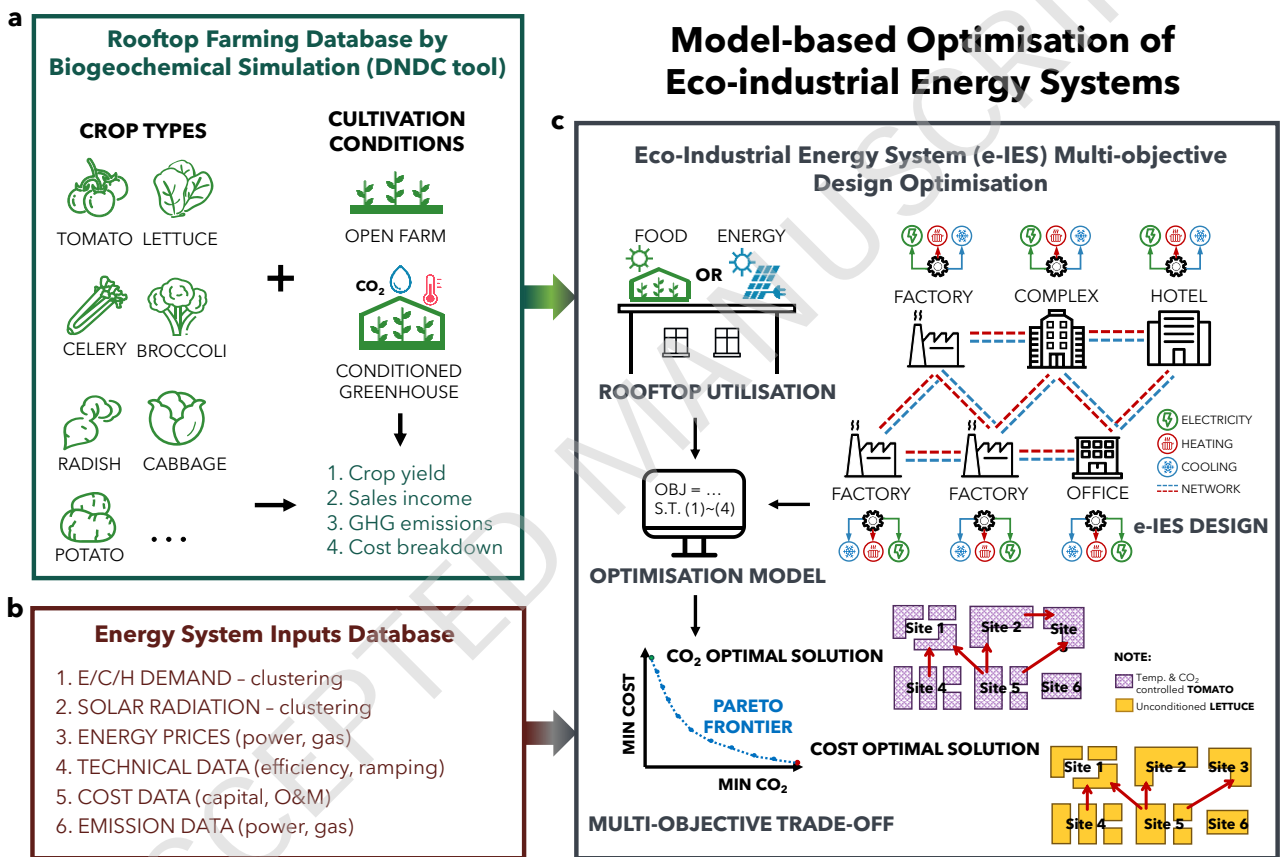


**Figure 1 Outline of the model-based optimisation of eco-Industrial Energy System (e-IES) design.** **a**, rooftop farming database including yield cost and emissions achieved by the DeNitrification-DeComposition (DNDC) tool; **b**, energy system related inputs where the clustering technique is applied when necessary; **c**, multi-objective e-IES design and rooftop utilisation optimisation resulting in a series of Pareto optimal solutions.

## 2.1 Rooftop farming database by Biogeochemical simulation

The rooftop farming database was developed by adopting the DNDC model presented in our previous research [27]. In contrast to data-driven empirical models, DNDC is underpinned by first-principle modelling and simulates biogeochemical processes. DNDC is

one of the most widely adopted biogeochemistry models first proposed by Li et al. [26] and has been validated worldwide including projection of vegetable growth in different regions and environments, e.g., in China [28] and in Ghana [29]. DNDC has experienced over two-decade development a DNDC family tree is presented by the comprehensive review by Gilhespy et al. [30]. A complete suite of biogeochemical processes (e.g., plant growth, organic matter decomposition, fermentation, ammonia volatilisation, nitrification, denitrification) is embedded in the DNDC model, enabling computation of carbon and nitrogen transport and transformations in plant-soil ecosystems. DNDC consists of two components. The first component, consisting of the soil climate, crop growth, and decomposition sub-models, transforms primary drivers (e.g., climate, soil properties, vegetation, and anthropogenic activity) to soil environmental drivers (e.g., temperature, moisture, pH, redox potential, and substrate concentration gradients). The second component, including the nitrification, denitrification, and fermentation sub-models, simulates C and N transformations mediated by the soil microbes [31].

As illustrated by Figure 1, DNDC was informed by integrating whole-year daily climate data to simulate the daily incremental growth of the living plants on rooftop under different conditions where not only natural conditions but also the enhanced photosynthetic assimilation of CO<sub>2</sub> in response to elevated CO<sub>2</sub> concentration under greenhouse were modeled [32]. This study simulates seven vegetable crops (i.e., tomato, lettuce, celery, broccoli, radish, cabbage, and potato) cultivated under open farm and conditioned greenhouse. Nine different greenhouse conditions were simulated by configuring temperature levels (i.e., 20 °C, 23 °C, and 26 °C) and carbon dioxide concentrations (i.e., 350 ppm, 450 ppm, and 550 ppm). Thus, ten rooftop crop cultivation conditions (1 open farm and 9 conditioned greenhouse) form a comprehensive database consisting of 70 datasets as visualised in Figure 2. The climate data including daily temperature and precipitation are derived from the average of 3-year daily meteorological data, which can be obtained from the meteorological data sharing service system [33] and given in Appendix Figure A1.

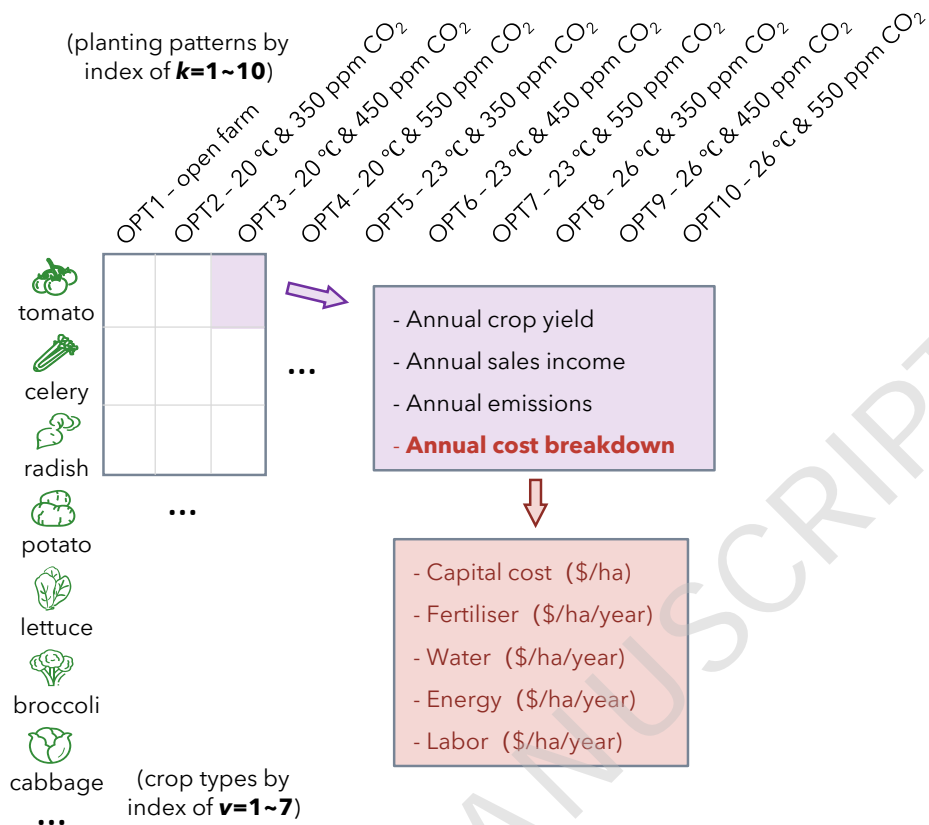


**Figure 2 Rooftop farming database structure with data definitions and dataset identifiers.**

## 2.2 Schematic of an eco-industrial energy system

A multi-energy system was considered that fulfills electricity, cooling, and heating demand of an industrial park, as illustrated in Figure 3. Each site was modelled to build its own multi-energy system and energy network connections among sites were also enabled. By further enabling rooftop farming, an e-IES design optimisation model was developed to optimise the rooftop utilisation options, e-IES systematic configurations, energy (i.e., cooling and heating) network connections, and the e-IES operational strategies simultaneously.

In the e-IES model, the whole year has been divided into three representative seasons, i.e., summer, winter, and transition season [34]. Summer associates with significant amount of cooling demand and less heating demand (for hot water supply); winter associates with significant amount of heating demand and less cooling demand (for conditioned workshops); transition season (spring and fall) associates with both less cooling and heating demand as no general space cooling and heating requirement. Each representative season was assigned with different number of days. A typical daily demand profile for each season was generated with an hourly temporal resolution, which enables optimisation model to capture the demand fluctuation. The entire model was formulated as a Mixed Integer Linear Programming (MILP)

optimisation problem based on previous work [35, 36].

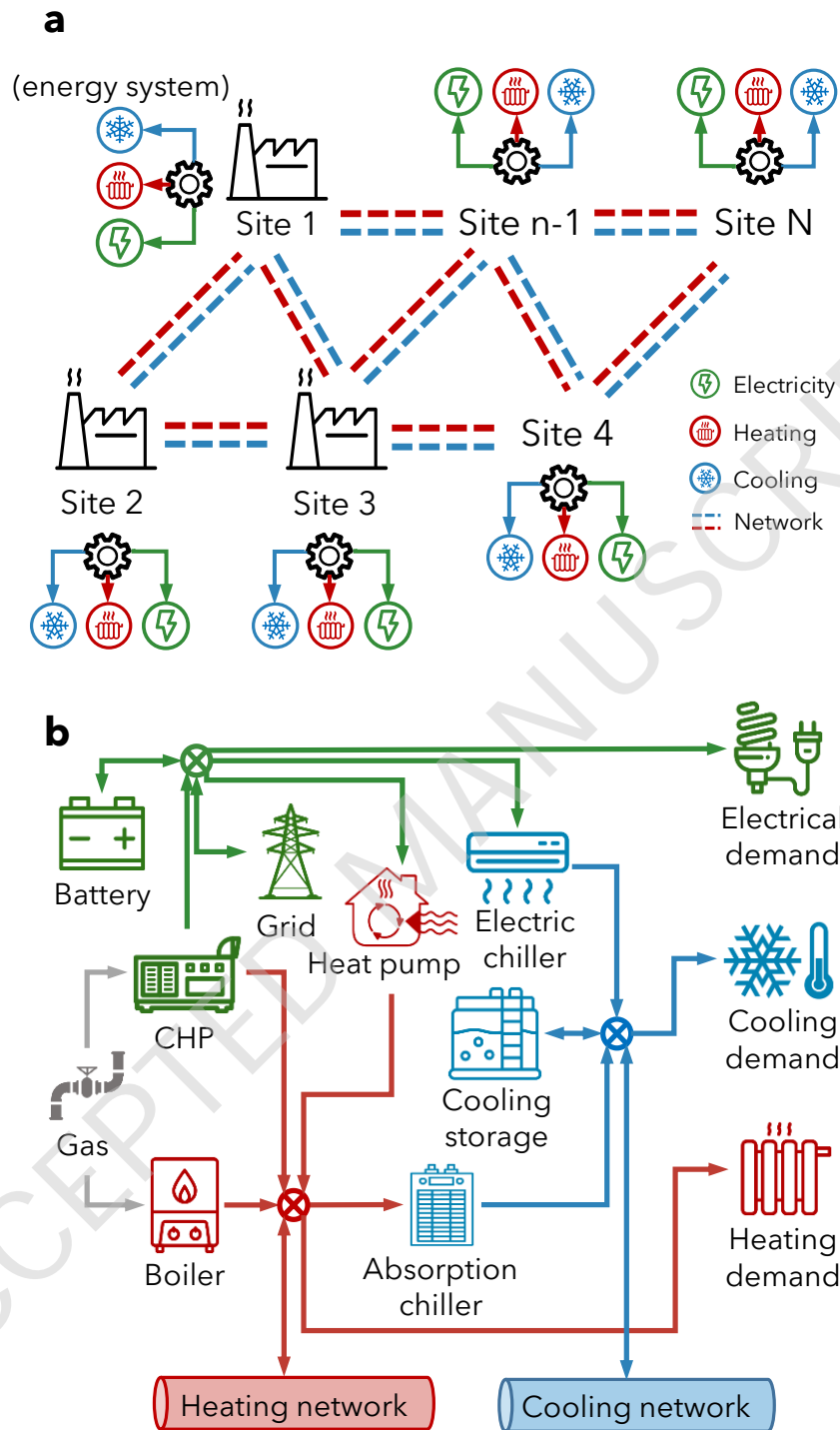


**Figure 3 Outline of the e-IES design optimisation model. a**, availability of energy network connection for each site's individual energy system; **b**, possible configurations for each individual energy system with cooling, heating, and electricity supply technologies.

### 2.3 Modelling framework and objective functions

In the e-IES design optimisation model, two conflicting objectives have been considered,

i.e., minimised the total annualised cost (TAC) over 20-year horizon, and minimised the annualised CO<sub>2</sub>-equivalent emissions (ACE) of the e-IES. The epsilon-constraints based multi-objective optimisation method has been applied in this study to address the trade-off between two conflicting objectives for e-IES design [37].

The two objectives, a range of energy system constraints, and logical constraints for rooftop option choices have been outlined below. More detailed constraint formulations can be found in **Appendix A.1** and the model parameterisation is given in **Appendix A.2**.

**Min**  $obj_1$  = total annualised cost (TAC) by Eq. 1~8

**Min**  $obj_2$  = annualised CO<sub>2</sub>-equivalent emissions (ACE) by Eq. 9

**S.T.** Energy balances

Rooftop options constraints

Conversion constraints

Capacity expansion constraints

Operation constraints

Cooling storage constraints

Battery storage constraints

Grid connection constraints

Energy network constraints

The total annualised cost (TAC) objective function is defined in **Eq. 1**. In addition to energy technologies, our research also considers the capital and O&M cost as well as the yield income of an e-IES.

$$TAC = CAPEX + FC + MC + GC + YI \quad (1)$$

where *CAPEX* represents the capital cost for both energy technologies and rooftop farming settings, *FC* denotes the fuel cost, *MC* is the maintenance cost, *GC* is the grid cost, and *YI* is the farming yield income.

The *CAPEX* accounts for the investment on energy devices, energy networks, and construction of different rooftop farming settings, see Eq. (2). The *CAPEX* is further annualised by multiplying a capital recovery factor (*CRF*) assuming the interest rate of 5%, see Eq. (3). The service life of energy devices and rooftop farming settings is assumed as 20 and 15 years, respectively, and energy network is assumed with 30 years' service life. Eq. (4) constrains the number of crop and cultivation condition selected for each rooftop agricultural cultivation site.

$$\begin{aligned}
CAPEX = & \sum_i \sum_t CAP_{i,t} \times C_t^{CAP} \times CRF_t + \sum_i \sum_j DX_{i,j} \times C_{pipe}^{CAP} \times CRF_{pipe} \\
& + \sum_v \sum_k \sum_i \varphi_{i,v,k}^{RF} \times C_{v,k}^{CAP} \times CRF_{RF} \quad \forall j > i
\end{aligned} \tag{2}$$

$$CRF = \frac{r \times (1+r)^n}{(1+r)^n - 1} \tag{3}$$

$$\sum_{v=1}^7 \sum_{k=1}^{10} \varphi_{i,v,k}^{RF} \leq 1 \tag{4}$$

where  $i, j, t$  denotes site number ( $i$  and  $j$ ), and energy technologies ( $t$ ), respectively;  $k=1\sim 10$  denotes 10 rooftop cultivation conditions;  $v=1\sim 7$  represents 7 crop options.  $CAP$  indicates the installed capacity of energy devices.  $DX$  represents the distance between sites.  $\varphi$  is a binary variable controlling the selection of one certain crop and one cultivation condition on the rooftop of one site.

Fuel cost ( $FC$ ) is defined by the gas consumption cost by the Boiler and the CHP (Eq. (5)).

$$FC = \sum_i \sum_s \sum_h \left[ \left( \frac{E_{i,s,h}^{CHP}}{\eta^{CHP}} \times C_h^{CHP-NG} + \frac{Q_{i,s,h}^B}{\eta^B} \right) \times C_h^{B-NG} \right] \tag{5}$$

where  $i, s, h$  denotes the sites, seasons, and hours, respectively.  $E^{CHP}$  is the electricity generated by CHP,  $Q^B$  indicates the heating generated by boiler,  $\eta$  is the efficiency, and  $C^{CHP-NG}$  and  $C^{B-NG}$  are the unit cost of natural gas, which could be different depending on local policies.

As given in Eq. (6), maintenance costs ( $MC$ ) includes annual MC for rooftop farming options and MC for energy devices, which is determined by the product of energy output from each device and the corresponding unitary maintenance cost ( $C^{maint}$ ).

$$MC = \sum_i \sum_s \sum_h (E_{i,s,h}^{CHP} + Q_{i,s,h}^{HP/B-heat} + Q_{i,s,h}^{E-CH/A-CH} + Q_{i,s,h}^{st} + E_{i,s,h}^{st}) \times C_t^{maint} + \sum_i \sum_v \sum_k C_{i,v,k}^{RF} \tag{6}$$

where  $E^{CHP}$  is electricity generated by CHP;  $Q^{E-CH/A-CH}$  is cooling energy generated by electric chiller or absorption chiller;  $E^{st}$  and  $Q^{st}$  are cooling and electricity been stored, respectively; and  $C^{RF}$  is the annual maintenance cost of each rooftop farming option.

As defined in Eq. (7), grid cost ( $GC$ ) depends on the purchased electricity cost and the revenue generated by the selling surplus onsite electricity back to the grid.

$$GC = C_h^{im} \times \sum_i \sum_s \sum_h E_{i,s,h}^{im} - C_h^{ex} \times \sum_i \sum_s \sum_h E_{i,s,h}^{ex} \tag{7}$$

where  $C^{\text{im}}$  and  $C^{\text{ex}}$  are the tariff for buying and selling electricity back to grid, respectively.  $E^{\text{im}}$  and  $E^{\text{ex}}$  represent the amount of electricity purchased and sold.

Yield income ( $YI$ ) is calculated by the income of selling yields from the rooftop farming (Eq. (8)).

$$YI = \sum_i \sum_v \sum_k \varphi_{i,v,k}^{\text{RF}} \times \text{sales}_{i,v,k} \quad (8a)$$

$$\text{sales}_{i,v,k} = C_v^{\text{RF}} \times A_i \times \text{yield}_{v,k} \quad (8b)$$

where  $\varphi$  is a binary variable for the selection of crop ( $v$ ) and cultivation condition ( $k$ ),  $\text{sales}_{i,v,k}$  represents the annual income per site for different rooftop farming options,  $C^{\text{RF}}$  is the unit price of each crop,  $A_i$  is the available rooftop area of each site, and  $\text{yield}_{v,k}$  is the simulated yield of each crop under different cultivation conditions.

The annualised carbon emissions ( $ACE$ ) objective function not only accounts for the carbon profiles of energy technologies but also capture the carbon nitrogen cycles and reflect the net carbon emissions from rooftop farming system, Eq. (9a~d).

$$ACE = NGE + GEE + RFE \quad (9a)$$

$$NGE = \psi_{\text{NG}} \times \sum_i \sum_s \sum_h \left( \frac{E_{i,s,h}^{\text{CHP}}}{\eta^{\text{CHP}}} + \frac{Q_{i,s,h}^{\text{B}}}{\eta^{\text{B}}} \right) \quad (9b)$$

$$GEE = \psi_{\text{grid}} \times \sum_i \sum_s \sum_h E_{i,s,h}^{\text{im}} \quad (9c)$$

$$RFE = \sum_i \sum_v \sum_k \psi_{v,k}^{\text{RF}} \times A_i \times \varphi_{i,v,k}^{\text{RF}} \quad (9d)$$

where  $NGE$ ,  $GEE$ , and  $RFE$  are the natural gas emissions, grid electricity emissions, and rooftop farming emissions;  $\psi_{\text{NG}}$ ,  $\psi_{\text{grid}}$  and  $\psi^{\text{RF}}$  are the GHG emission factor for natural gas, utility grid, and different rooftop farming options, respectively, where negative emissions could be induced by rooftop farming options due to the carbon sequestration;  $E^{\text{CHP}}$  and  $Q^{\text{B}}$  are the electricity generated by CHP and heating generated by boiler, respectively;  $\eta$  defines the efficiency;  $E^{\text{im}}$  is the amount of purchased electricity;  $A_i$  represents the available rooftop area of each site; and  $\varphi$  is a binary variable ensuring on more than one crop and cultivation system is selected for each site. The GHGs of rooftop agriculture represents the land use GHGs. It accounts for the carbon cycles in agro-ecosystem including the crop photosynthesis-fixed carbon, plant respiration (root, shoot and leaf) and microbial heterotrophic respiration to convert soil organic carbon to GHGs. However, the operational and capital GHGs embedded in fertiliser, energy and greenhouse materials, as well as downstream GHGs at

crop consumption and disposal phases were not accounted for. The GHGs of energy systems focuses on operational emissions without considering the GHGs embedded in capital inputs e.g. PV panel material, boilers, chillers material inputs, pipeline building materials.

## **2.4 Clustering technique**

To enable the optimisation model computationally intractable, the widely applicable clustering technique, i.e. k-medoids clustering method [38], was adopted to cluster representative demand profiles [6] in accordance with the model's temporal settings.

## **2.5 Computational method**

The epsilon-constraints based multi-objective optimisation method has been applied to address the system design trade-offs between the cost minimum and GHG minimum objectives [36]. The mathematical MILP optimisation model in this study is formulated in GAMS [39] and is resolved using CPLEX 28.2 solver on an Intel(R) Core(TM) i7-8565U CPU @1.8 GHz with 8GB of memory. The CPLEX solver is widely adopted to solve MILP problems and its robustness and efficiency have been demonstrated in previous research [40]. The e-IES optimisation model with  $2.8 \times 10^5$  variables ( $1.4 \times 10^5$  are binary) was resolved in approximately 45 min CPU time at an optimality gap of 2%.

## **3 Case study setups with clustered demand data**

An industrial park located in Suzhou city with six different sites (see Figure 4a) has been used as an optimisation case study. Suzhou is a major city located in the Yangtze River Delta, China, characterised with hot summer and cold winter. In the industrial park, all buildings offer sufficient structural strength to develop rooftop farming. Several buildings while located within one factory border are considered as one site. Each site has different rooftop available areas (see Figure 4b), and the demand patterns for each site are different so that energy networking availabilities may potentially save energy bills due to the demand complementarity over the same time horizon.

The typical hourly energy (cooling, heating, and electricity) demand profiles for six sites are obtained by clustering the 2-year (2016 and 2017) historical measurement data and presented in Figure 5. When rooftop farming is applied, the heat transfer coefficient of building rooftops and local micro-climate will change [41]; open farm and greenhouse are expected to affect building thermal demands to different extents. Based on the method in Ref. [42], the cooling and heating demand profiles are estimated to scale down 4% and 6% by implementing open farm and greenhouse on rooftops, respectively.

In addition, the parameters corresponding to each simulated crop in this study are listed in Table 1. The maximum biomass yield, the biomass fraction and the carbon to nitrogen ratios are key inputs associated with the simulated biomass for grain, leaf, stem, and root of a crop. The thermal degree day refers to cumulative air temperature from seeding until maturity of a crop. The tillage and fertilising methods vary with different crops [43].

ACCEPTED MANUSCRIPT

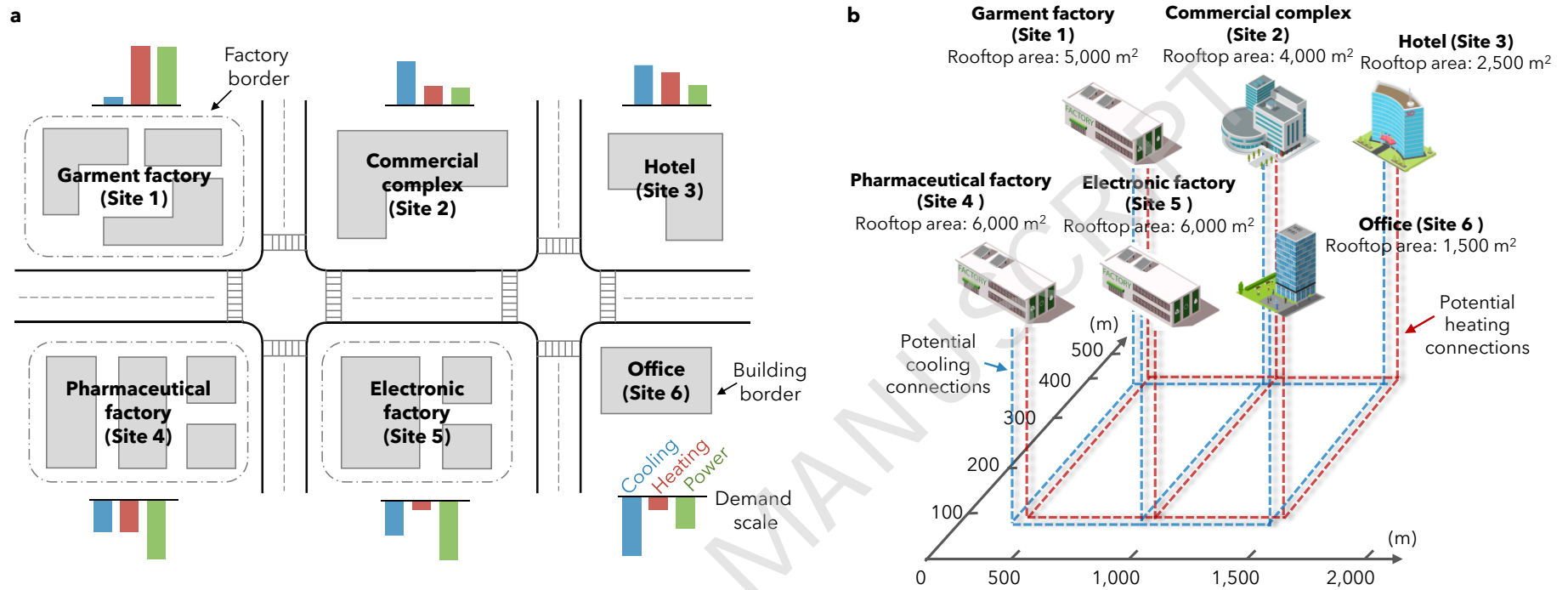


**Figure 4** The case study industrial park including six sites with varying energy demand scales and rooftop areas. **a**, six sites all have different energy demand scales; **b**, location map of six sites with rooftop areas and illustration of potential energy (i.e., cooling and heating) network connections.

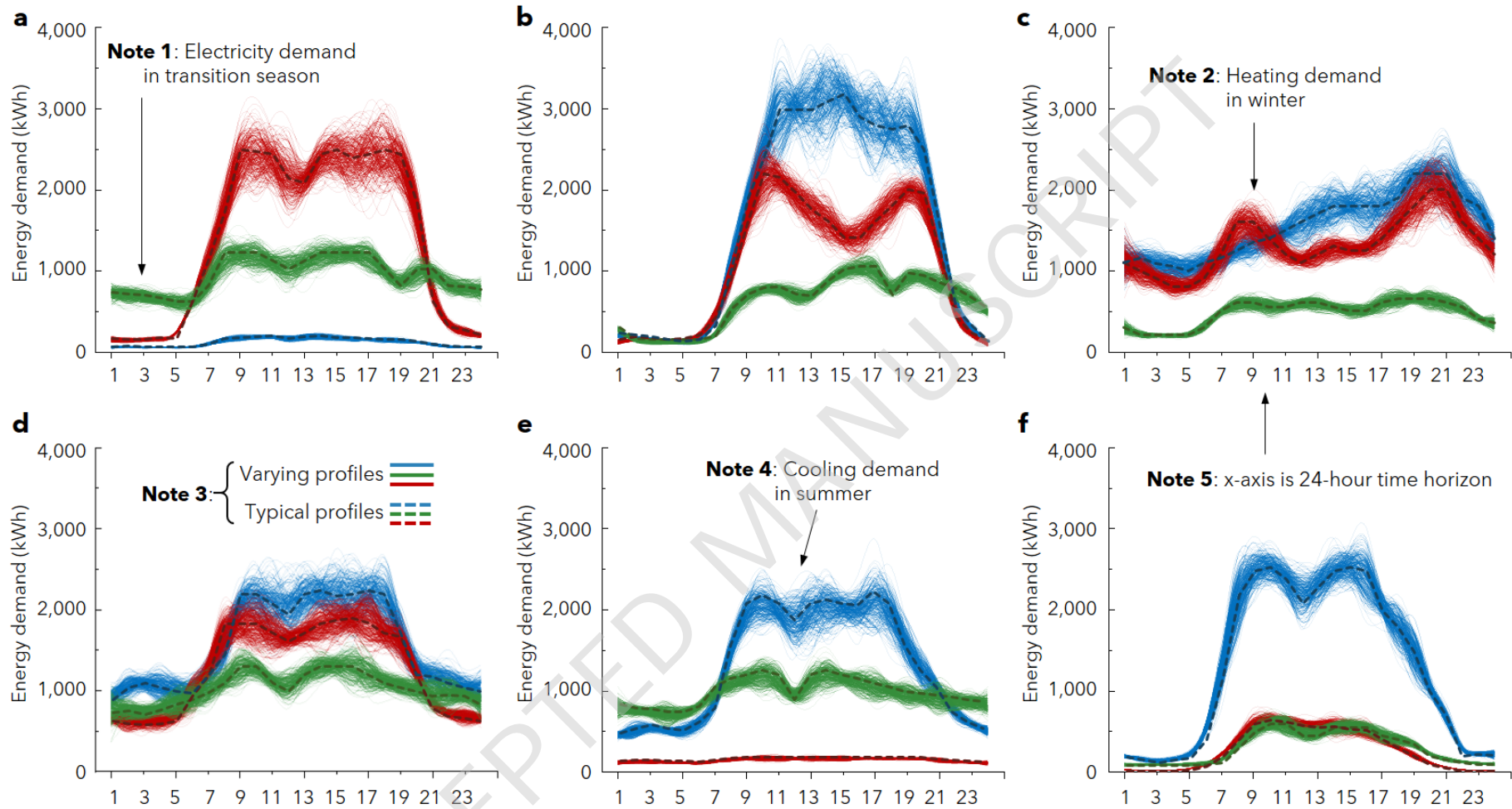


**Figure 5 Typical energy demand profiles (cooling in summer, heating in winter, electricity in transition seasons) for six sites. a, the garment factory (site 1); b, the commercial complex (site 2); c, the hotel (site 3); d, the pharmaceutical factory (site 4); e, the electronic factory (site 5); f, the office (site 6).**

**Table 1 Physiological parameters of all simulated crops**

Settings	Maximum biomass yield (kg/C/ha/yr)	Biomass fraction (seed)	C/N ratio (seed)	Annual N demand (kg N/ha/yr)	Thermal degree days (TDD)	Water demand (kg water/kg dry matter)
lettuce	914	0.64	11.5	100	1,400	800
broccoli	600	0.3	10	141	1,800	600
tomato	2010	0.36	26	197	1,400	900
cabbage	28	0.01	15	130	2,500	600
potato	2000	0.7	60	48	2,100	500
radish	1000	0.75	19	60	1,000	508
celery	40	0.01	12	289	1,300	500

## 4 Results and discussion

### 4.1 Rooftop farming yields and emissions

The rooftop farming database records the DNDC simulated data (crop yield and emissions) and economic data (cost and income). The cost data accounted for the capital costs and the operational costs for fertilisation (energy, agro-chemical, and labor cost), irrigation and other field management costs. Detailed cost data for different crops are presented in Appendix Table A5~A11. The income is calculated by the yield and the retail market price been presented in Table A12 in Appendix. Table 2 displays the annual crop yields based on DNDC simulated daily incremental growth. Among the 7 simulated crops, lettuce, tomato, and celery demonstrated the highest yields across a range of cultivation conditions. Table 3 summarises the simulated net ecosystem exchange (NEE) of carbon. NEE is equivalent to the difference between total amount of photosynthesis-fixed carbon and ecosystem respiration (i.e. biotic conversion of organic carbon to carbon dioxide by all organisms in the rooftop ecosystem accounting for plant respiration (root, shoot and leaf) and microbial heterotrophic respiration). Thus, NEE represents the net CO<sub>2</sub> emissions from biogeochemical carbon cycles in rooftop agricultural systems. A crop cultivation with a negative NEE value indicates net carbon sink effects therefore offers decarbonisation benefits.

As shown in Table 3, tomato delivered negative NEE across different cultivation options, where the NEE for other crops vary significantly with the options between open farm and conditioned greenhouse. NEE is not only regulated by plant physiological traits, photosynthesis pathways (e.g. Calvin-Benson-Bassham or C<sub>3</sub>, Hatch-Slack or C<sub>4</sub> cycles), but also affected by environmental variables (e.g. temperature, CO<sub>2</sub> level). Such trends can be observed from Table 3, NEE fluctuate with the temperature and elevated CO<sub>2</sub> concentration in greenhouse cultivation conditions. However, DNDC simulations including biogeochemical carbon and nitrogen cycles represent theoretical results derived from computational experiments; however, to further validate the applicability of such simulation model and advance the understanding of C and N cycling in rooftop agro-ecosystems, comparisons of DNDC simulation with measurement obtained from experiment field would be needed in future research.

**Table 2 Simulated annual yield for 7 crops under different cultivation conditions**

yield (kg/ha)	OPT1	OPT2	OPT3	OPT4	OPT5	OPT6	OPT7	OPT8	OPT9	OPT10
lettuce	117,288	224,585	249,563	254,125	240,875	252,387	253,907	243,482	250,649	255,428
broccoli	14,299	15,790	17,549	18,966	18,437	20,469	22,138	19,625	21,802	23,561
tomato	109,419	116,186	122,570	123,847	124,741	130,550	132,146	126,017	130,103	132,210
cabbage	24,309	79,410	88,223	95,338	94,098	104,518	112,964	101,856	113,147	114,524
potato	5,892	8,918	9,913	10,708	9,852	10,950	11,830	10,040	11,157	12,054
radish	62,805	83,085	99,800	102,396	76,907	85,452	99,755	66,232	73,598	79,520
celery	130,591	172,462	191,610	206,928	184,461	205,014	199,907	186,091	197,884	197,354

**Table 3 Simulated annual NEE for 7 crops under different cultivation conditions**

NEE (kg/ha)	OPT1	OPT2	OPT3	OPT4	OPT5	OPT6	OPT7	OPT8	OPT9	OPT10
lettuce	-1,666	1,404	1,000	990	1,001	810	785	955	828	759
broccoli	-753	6,227	5,246	4,588	6,096	5,138	42,92	6,196	5,184	4,439
tomato	-7,291	-8,746	-9,046	-9,405	-4,910	-4,872	-4,992	-4,560	-4,909	-5,085
cabbage	15	-2,872	-838	-1,638	-1,219	-2,032	-1,800	-1,858	-3,067	-3,286
potato	-4,647	10,969	9,798	8,582	10,465	9,071	8,116	10,582	9,355	8,324
radish	-5,200	16,239	14,758	18,395	18,395	17,178	13,456	20,588	19,372	18,541
celery	-4571	5,877	4,847	4,028	3,138	1,857	2,137	5,394	5,030	4,764

## 4.2 Optimal rooftop options and corresponding e-IES design

By solving the e-IES optimisation model, optimal rooftop design strategies can be achieved. The pareto frontier presented in Figure 6a shows a set of non-dominated optimal solutions to address the design trade-offs between cost and GHG emission reduction objectives. The least TAC solution achieved the least total annualised cost (TAC) of  $2,437 \times 10^3$  US\$/year with  $237 \times 10^3$  ton/year GHG emissions; in contrast the emission-least solution delivered a low-carbon profile with  $131 \times 10^3$  ton/year annualised GHG emissions but with the higher cost of  $3,727 \times 10^3$  US\$/year.

The least TAC solution selects to plant lettuce with open farm cultivation option. With the optimal solutions shifting from the least cost to the least emissions, the rooftop farming decisions showed a transition from lettuce plantation under conditioned greenhouse (i.e., 20 °C and 550 ppm CO<sub>2</sub>) to open farming of tomato, and finally to tomato plantation under conditioned greenhouse (i.e., 20 °C and 550 ppm CO<sub>2</sub>). It is interesting to observe that although the NEE performance in Table 3 shows “lettuce unconditioned” (OPT1) is beneficial for carbon emissions than “lettuce in greenhouse” (OPT4), the OPT4 still indicates a lower emission solution. This is due to assumption that greenhouse could directly reduce more cooling and heating demand of the sites than unconditioned open farm as denoted in Table A4, and such direct energy demand reduction led by rooftop farming plays a more dominant role than the NEE in this situation, which also reveals that the interlink between rooftop farming and the whole system design are comprehensive and the proposed model is therefore of importance to quantify such an interlink.

Meanwhile, a general trend in energy network decisions was observed, i.e. more active transfer of the heating energy among sites than the cooling energy. This was driven by the modelling configuration which enabled cooling storage for each site, so that cooling energy can be stored and utilised locally other than transferred to neighboring sites. Notably, Site 5 (i.e. the electronic processing site) has been selected to output heating energy to neighboring sites across the Pareto optimal solutions. This can be explained by the relatively low heating demand but high electricity requirement in Site 5 as illustrated in Figure 5; thus, to meet Site 5’s electricity demand, the combined heating and power (CHP) technology would generate a significant amount of surplus heating, which can be transferred to neighboring sites.

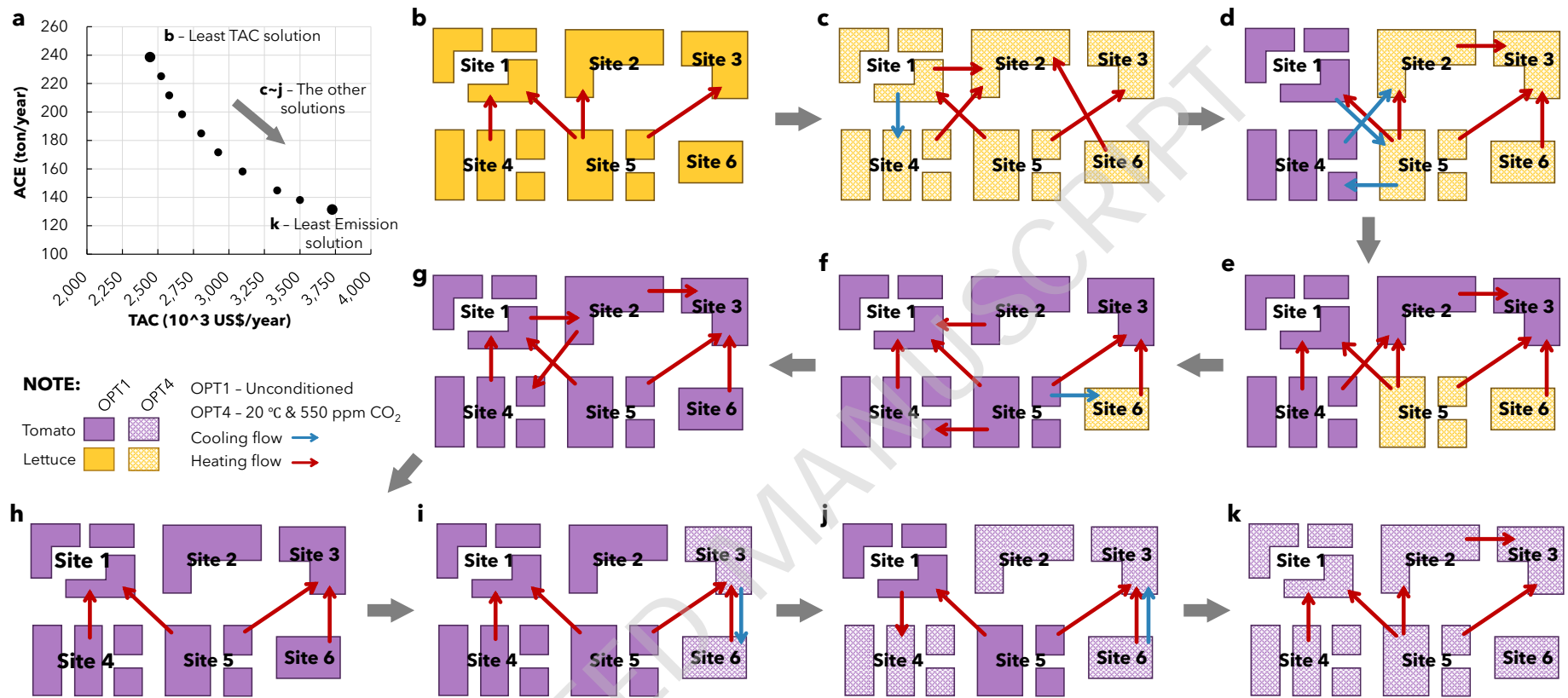


**Figure 6 Optimal design for e-IES considering trade-offs between cost and emission objectives and corresponding rooftop options and energy network design. a, Pareto frontier showing design trade-offs; b, rooftop options and energy flow for the least TAC solution; c~j, rooftop options and energy flow for the other solutions; k, rooftop options and energy flow for the least emission solution.**

Figure 7 further shows the comparison of system configurations for the least TAC solution in contrast to the least emission solution. The six sites' system configurations are optimised simultaneously considering both energy network design and rooftop farming solutions (as reported in Figure 6). For both solutions, no battery storage was adopted due to the relatively high capital costs; and the boiler capacity design was small as CHP could provide heating by utilising the residual heat along with power generation. The least TAC solution selected to install larger CHP capacities for each site to efficiently utilise residual heat to meet heating demands, whereas much lower heat pump (HP) capacity was selected. Meanwhile, the residual heat can be utilised by the relatively high capacity of absorption chiller (A-CHILLER) to provide cooling so that less capacity of electric chiller (E-CHILLER) was selected for the least TAC solution. Since the cooling generated by residual heat and cooling demand could mismatch, larger capacity of cooling storage was needed in the least TAC solution.

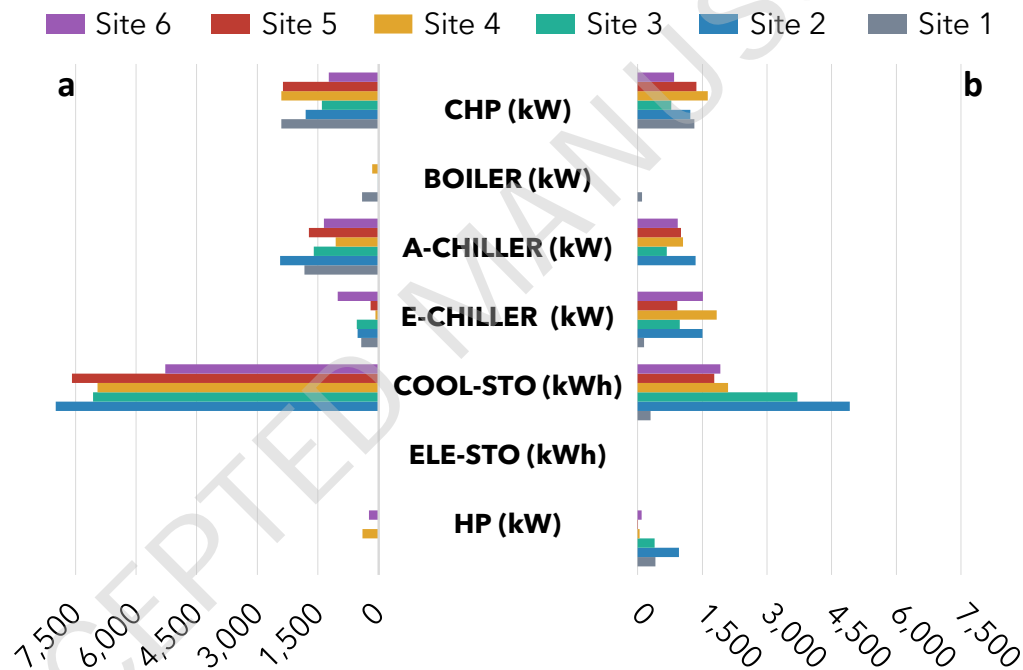


**Figure 7 Comparison of the six sites' system configurations between the least TAC solution and the least emission solution. a, least TAC solution; b, least emission solution.** Abbreviation: CHP (combined heating and power), A-CHILLER (absorption chiller), E-CHILLER (electric chiller), COOL-STO (cooling storage), ELE-STO (battery storage), HP (heat pump).

### 4.3 Comparison with rooftop photovoltaic (PV) and spare roof

Figure 8 shows the comparison between optimal solutions achieved with rooftop farming options with the set of optimal solutions derived from two other rooftop utilisation scenarios, i.e., rooftop PV option and unused rooftop. For the scenario of rooftop PV option, the capital and O&M costs of the rooftop PV system need to be considered, and renewable solar power

is generated with less emissions and may save the fuel consumption of the energy system. The capital and O&M costs as well as the emissions induced by the rooftop farming options need to be deducted from the objective functions. As for the unused rooftop scenario, all energy, cost and emission terms associated with either rooftop farming or PV are deducted from the objective functions. Therefore, when generating the set of optimal solutions for rooftop PV and unused rooftop scenarios, a slightly adjustment is needed for the TAC and ACE objective functions as presented in Eq. 1~8 and Eq. 9, respectively.

In general, implementing rooftop farming enabled both cost savings and decarbonisation compared to rooftop PV and unused rooftop scenarios, though the rooftop PV and rooftop farming deliver similar performance while achieving the least cost solution. Such observation is case specific, the regions with higher solar resource might result in rooftop PV as cost-optimal solution. Meanwhile, more saving effects were observed in the solution comparisons for the GHG emission reduction (i.e., 16% and 10.2%) than the cost benefit (5.6% and 2.4%). Such a trend indicated that implementing rooftop farming delivered higher benefits from the environmental perspective than the economic perspective. The Pareto optimal solutions with rooftop farming achieved higher savings in comparisons with the scenarios with unused rooftop (i.e., 5.6% for cost and 16.3% for GHG emissions) than scenarios with the rooftop PV (i.e., 2.4% for cost and 10.2% for GHG emissions). This observation provides evidence for future rooftop utilisation decision-making: rooftop utilisation by either energy or farming systems is worth further investigation from both economic and environmental perspectives.

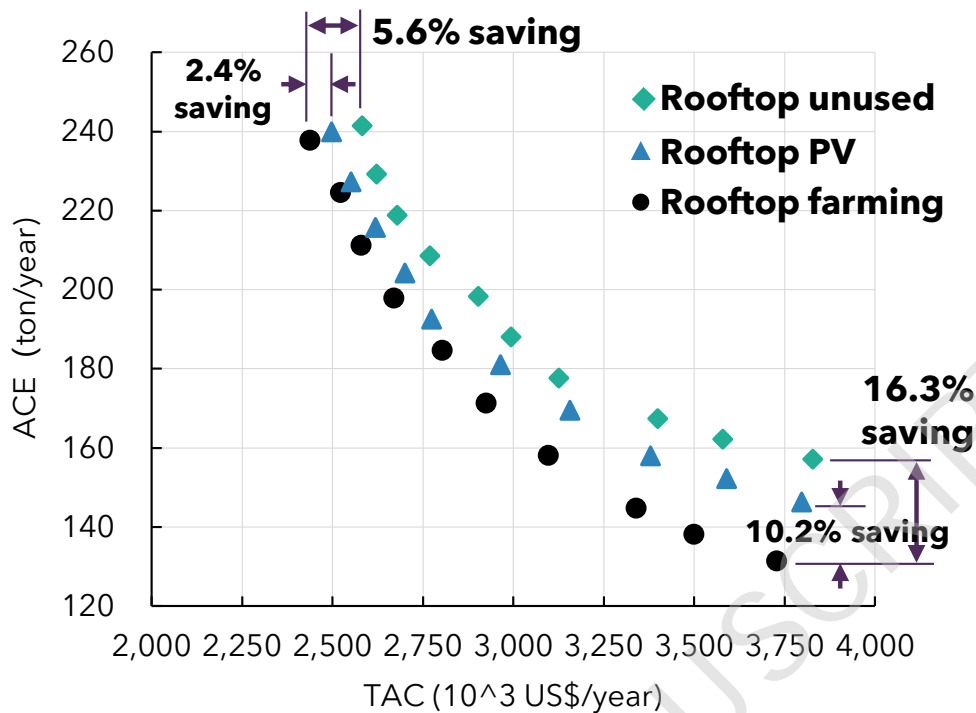


**Figure 8 Optimal solution comparisons among rooftop farming, PV rooftop, and spare rooftop scenarios.** Abbreviation: ACE – annualised carbon emission, TAC – total annualised cost.

#### 4.4 Limitations and the way forward

This study presented a biogeochemical simulation and energy system integrated model towards eco-industrial energy system optimisation.

Research limitations and emerging research directions are highlighted below:

- Rooftop agriculture GHGs induced by land use effects and agro-ecosystem biogeochemical processes have been captured. Such GHGs include the crop photosynthetic carbon sequestration (negative GHG emissions) and emissions released to atmosphere due to plant respiration as well as soil microbiome respiration. However, in future research, it is worth to couple full life cycle approach with the develop IES model to account for operational and capital GHGs at rooftop agriculture stage such as GHGs embedded in greenhouse materials or field operations.
- The land-use GHGs derived from DNDC simulation represent theoretical values and computational experiments which would need further validation by comparing with field measurements. Another interesting direction would be to couple computational and field experiments to explore the possibility to use organic fertilisers derived from IES system e.g. organic waste from food industry or local sanitation systems in agriculture practice. This would lead to a resource-circular zero-waste IES optimisation and design problem.

- c) This study presents a deterministic optimisation problem, the data variability and uncertainty in biogeochemical simulation and energy system model were not considered in current study. However, in future, it is worth to expand the optimisation framework to explore nonlinearity and uncertainty. Global sensitivity analyses, e.g., screening methods, regression-based approach or variance-based methods represent potential directions to advance the understanding of how input variation affect modelling evidences. Optimisation under uncertainty would be another direction worth exploring. In addition, it would be interesting to couple global sensitivity analyses and meta-modelling with our developed IES model to enable computational efficient way to incorporate the approximate mathematical representation of complex simulators e.g. DNDC into eco-industrial energy optimisation.
- d) The framework is featured by extensibility, adoptability, and scalability. The optimisation framework model can be potentially expanded to incorporate above-mentioned sensitivity analysis, in-depth scenario analyses, e.g., rooftop farming effects on local thermal demands and cover a broader scope of project lifecycle to inform decision-making. Model scalability is reflected by wider application in use cases. The rooftop farming concept and the proposed model could be adapted and scaled to large-scale case studies beyond industrial parks such as region-level urban communities or business zones. The framework is expected to benefit wider stakeholders, e.g., industrial park designer or urban planners, to inform decision-making on, e.g., design options for energy-system decarbonisation. Beyond the region presented in current study, the developed framework could be applied to other countries or regions by considering local technical, economic, and environmental characteristics.

## 5 Conclusions

To decarbonise the energy systems in process industry, this study presents a nexus design by integrating rooftop farming into process industrial energy system optimisation. A model-based e-IES design optimisation framework is therefore proposed, which couples first-principle underpinned simulation, clustering algorithms, and mathematical optimisations. Within the framework, a rooftop farming database derived from computational simulation and clustered energy system data were generated to inform the optimisation model for optimal design of the eco-industrial energy system (e-IES) and the functional rooftop utilisation.

The framework was applied to inform the e-IES decision-making under the context of an industrial park in China. Generally, implementing rooftop farming could generate mutual benefits from both cost and carbon emission reduction perspectives when compared to either rooftop PV or unused rooftop. Significant benefit can be expected from decarbonisation perspective in comparison with economic benefits. The derived Pareto optimal solutions showed that lettuce cultivation under open farm represented the least cost option; while planting tomato in controlled greenhouse with elevated CO<sub>2</sub> concentration (i.e., 20 °C and 550 ppm CO<sub>2</sub>) could achieve the least GHG emission solution.

The proposed modelling framework can be further extended to inform wider design case studies. Building on the proposed modelling framework, future research frontiers are to harness AI and data advances e.g. advanced learning algorithms for data analyses and hybrid search methods coupling exact and metaheuristic algorithms for responsive optimisation.

## **Acknowledgement**

J.L. would like to thank for the support from the National Natural Science Foundation of China (71573242). M.G. would like to acknowledge the UK Engineering and Physical Sciences Research Council (EPSRC) for providing financial support for research [EP/N034740/1], which forms fundamental research underpins part of this study.

## **Declaration of interest**

There are no conflicts to declare.

## **Reference**

- [1] IRENA. Reaching Zero with Renewables: Eliminating CO<sub>2</sub> emissions from industry and transport in line with the 1.5oC climate goal. International Renewable Energy Agency, Abu Dhabi. 2020 [Access: 2019/12/01]; [www.irena.org/publications](http://www.irena.org/publications).
- [2] Committee on Climate Change. Reducing UK emissions 2018 Progress Report to Parliament. 2018.
- [3] European Commission. Communication from the commission to the european parliament, the council, the european economic and social committee and the committee of the regions. 2011. [Access 2019/12/01].
- [4] Zhang X, Zhao X, Jiang Z, Shao S. How to achieve the 2030 CO<sub>2</sub> emission-reduction targets for China's industrial sector: Retrospective decomposition and prospective trajectories. *Global Environmental Change*. 2017;44:83-97.

- [5] Jing R, Wang M, Liang H, Wang X, Li N, Shah N, et al. Multi-objective optimization of a neighborhood-level urban energy network: Considering Game-theory inspired multi-benefit allocation constraints. *Applied Energy*. 2018;231:534-48.
- [6] Wang M, Yu H, Jing R, Liu H, Chen P, Li C. Combined multi-objective optimization and robustness analysis framework for building integrated energy system under uncertainty. *Energy Conversion and Management*. 2020;208:112589.
- [7] Jing R, Wang M, Zhang Z, Wang X, Li N, Shah N, et al. Distributed or centralized? Designing district-level urban energy systems by a hierarchical approach considering demand uncertainties. *Applied Energy*. 2019;252:113424.
- [8] Liu X, Yan Z, Wu J. Optimal coordinated operation of a multi-energy community considering interactions between energy storage and conversion devices. *Applied Energy*. 2019;248:256-73.
- [9] Perera ATD, Nik VM, Chen D, Scartezzini J-L, Hong T. Quantifying the impacts of climate change and extreme climate events on energy systems. *Nature Energy*. 2020.
- [10] Martín M, Grossmann IE. Optimal integration of a self sustained algae based facility with solar and/or wind energy. *Journal of Cleaner Production*. 2017;145:336-47.
- [11] Wu L, Liu Y, Liang X, Kang L. Multi-objective optimization for design of a steam system with drivers option in process industries. *Journal of Cleaner Production*. 2016;136:89-98.
- [12] Lee I, Tester JW, You F. Systems analysis, design, and optimization of geothermal energy systems for power production and polygeneration: State-of-the-art and future challenges. *Renewable and Sustainable Energy Reviews*. 2019;109:551-77.
- [13] Zhu X, Yang J, Pan X, Li G, Rao Y. Regional integrated energy system energy management in an industrial park considering energy stepped utilization. *Energy*. 2020;201:117589.
- [14] Shen F, Wang M, Huang L, Qian F. Exergy analysis and multi-objective optimisation for energy system: a case study of a separation process in ethylene manufacturing. *Journal of Industrial and Engineering Chemistry*. 2020.
- [15] Noorollahi Y, Golshanfard A, Aligholian A, Mohammadi-ivatloo B, Nielsen S, Hajinezhad A. Sustainable Energy System Planning for an Industrial Zone by Integrating Electric Vehicles as Energy Storage. *Journal of Energy Storage*. 2020;30:101553.
- [16] Wu N, Zhan X, Zhu X, Zhang Z, Lin J, Xie S, et al. Analysis of biomass polygeneration integrated energy system based on a mixed-integer nonlinear programming optimization method. *Journal of Cleaner Production*. 2020;271:122761.
- [17] Kotzur L, Markewitz P, Robinius M, Stolten D. Impact of different time series aggregation methods on optimal energy system design. *Renewable Energy*. 2018;117:474-87.
- [18] Benabdellah AC, Benghabrit A, Bouhaddou I. A survey of clustering algorithms for an industrial context. *Procedia Computer Science*. 2019;148:291-302.
- [19] Wang W, Jing R, Zhao Y, Zhang C, Wang X. A load-complementarity combined flexible clustering approach for large-scale urban energy-water nexus optimization. *Applied Energy*. 2020;270:115163.
- [20] Voulis N, Warnier M, Brazier FMT. Understanding spatio-temporal electricity demand at different urban scales: A data-driven approach. *Applied Energy*. 2018;230:1157-71.
- [21] Teichgraeber H, Brandt AR. Clustering methods to find representative periods for the optimization of energy systems: An initial framework and comparison. *Applied Energy*. 2019;239:1283-93.
- [22] Yilmaz S, Chambers J, Patel MK. Comparison of clustering approaches for domestic electricity

- load profile characterisation - Implications for demand side management. *Energy*. 2019;180:665-77.
- [23] Shen F, Zhao L, Du W, Zhong W, Qian F. Large-scale industrial energy systems optimization under uncertainty: A data-driven robust optimization approach. *Applied Energy*. 2020;259:114199.
- [24] Wang M, Yu H, Lin X, Jing R, He F, Li C. Comparing stochastic programming with posteriori approach for multi-objective optimization of distributed energy systems under uncertainty. *Energy*. 2020;210:118571.
- [25] Rajabi A, Eskandari M, Ghadi MJ, Li L, Zhang J, Siano P. A comparative study of clustering techniques for electrical load pattern segmentation. *Renewable and Sustainable Energy Reviews*. 2020;120:109628.
- [26] Li C, Frohling S, Frohling TA. A model of nitrous oxide evolution from soil driven by rainfall events: 1. Model structure and sensitivity. *Journal of Geophysical Research: Atmospheres*. 1992;97:9759-76.
- [27] Guo M, Li C, Facciotto G, Bergante S, Bhatia R, Comolli R, et al. Bioethanol from poplar clone Imola: an environmentally viable alternative to fossil fuel? *Biotechnol Biofuels*. 2015;8:1-21.
- [28] Wang Q, Liang X, Wang Y, Wang L, Mosier AR, Chen D. Assessment of nitrogen hotspots induced by cropping systems in the Bohai Rim region in China by integrating DNDC modelling and the reactive nitrogen spatial intensity (NrSI) framework. *Environmental Research Letters*. 2020;15:105008.
- [29] Budiman, Steiner C, Topp CFE, Buerkert A. Soil-climate contribution to DNDC model uncertainty in simulating biomass accumulation under urban vegetable production on a Petroplinthic Cambisol in Tamale, Ghana. *Journal of Plant Nutrition and Soil Science*. 2020;183:306-15.
- [30] Gilhespy SL, Anthony S, Cardenas L, Chadwick D, del Prado A, Li C, et al. First 20 years of DNDC (DeNitrification DeComposition): Model evolution. *Ecological Modelling*. 2014;292:51-62.
- [31] Guo M, Li C, Facciotto G, Bergante S, Bhatia R, Comolli R, et al. Bioethanol from poplar clone Imola: an environmentally viable alternative to fossil fuel? *Biotechnol Biofuels* 2015. p. 134.
- [32] Osborne CP. Crop yields: CO<sub>2</sub> fertilization dries up. *Nature Plants*. 2016;2:16138.
- [33] CMDC. China meteorological data sharing service system. <http://data.cma.cn>; 2018.
- [34] Gabrielli P, Furer F, Mavromatidis G, Mazzotti M. Robust and optimal design of multi-energy systems with seasonal storage through uncertainty analysis. *Applied Energy*. 2019;238:1192-210.
- [35] Jing R, Kuriyan K, Kong Q, Zhang Z, Shah N, Li N, et al. Exploring the impact space of different technologies using a portfolio constraint based approach for multi-objective optimization of integrated urban energy systems. *Renewable and Sustainable Energy Reviews*. 2019;113:109249.
- [36] Jing R, Hastings A, Guo M. Sustainable Design of Urban Rooftop Food-Energy-Land Nexus. *iScience*. 2020;23:101743.
- [37] Jing R, Zhu X, Zhu Z, Wang W, Meng C, Shah N, et al. A multi-objective optimization and multi-criteria evaluation integrated framework for distributed energy system optimal planning. *Energy Conversion and Management*. 2018;166:445-62.
- [38] Hoffmann MK, Leander; Stolten, Detlef; Robinius, Martin. A Review on Time Series Aggregation Methods for Energy System Models. *Energies*. 2020;13:641.
- [39] GAMS. A Users Guide. 2017. [Access: 2020/10/1].
- [40] IBM. CPLEX Optimization Studio. 2019.
- [41] Dong J, Lin M, Zuo J, Lin T, Liu J, Sun C, et al. Quantitative study on the cooling effect of green roofs in a high-density urban Area—A case study of Xiamen, China. *Journal of Cleaner Production*.

2020;255:120152.

[42] Zheng D, Yu L, Wang L, Tao J. A screening methodology for building multiple energy retrofit measures package considering economic and risk aspects. *Journal of Cleaner Production*. 2019;208:1587-602.

[43] Chen W. *Vegetable production technology*. Xiamen University Press. ISBN: 9787561545928. [In Chinese]. 2013.

[44] Jing R, Kuriyan K, Lin J, Shah N, Zhao Y. Quantifying the contribution of individual technologies in integrated urban energy systems – A system value approach. *Applied Energy*. 2020;266:114859.

ACCEPTED MANUSCRIPT

# Appendix

This appendix presents the model constraints in detail and all parameters that applied in the case study.

## A.1 Modelling constraints

The definitions of parameters and variables are given in Table A1~A3.

**Table A1 Definitions of indices**

Indices/subscript/ superscript	Definitions
$s$	Sets of three representative seasons
$h$	Sets of 24 hours
$i$	Sets of sites
$j$	Sets of sites, $j \neq i$
$t$	Sets of energy devices, including combined heating and power (CHP), boiler (b), electric chiller (E-CHILLER), absorption chiller (A-CHILLER), heat pump (hp), battery storage (ELE-STO), cooling storage tank (COOL-STO)
$v$	Sets of crops (tomato, lettuce, celery, broccoli, radish, cabbage, and potato)
$k$	Sets of three rooftop farming options ( $k=1$ open farming, $k=2\sim 10$ conditioned greenhouse with different temperature and indoor CO <sub>2</sub> control)

**Table A2 Definitions of parameters**

Parameters	Definitions
$C^{CAP}$	Unit capital cost [\$/kW] of energy technologies, heating and cooling network, and unit capital cost [\$/m <sup>2</sup> ] of rooftop farming option
$DX_{ij}$	Distance between sites
$\eta$	Efficiency of individual energy technology
H-to-P	Heat-to-power ratio of CHP
$C^{NG}$	Unit natural gas cost [\$/kWh]
$C^{maint}$	Maintenance cost [\$/kWh] of energy technologies
$C^{RF}$	Maintenance cost [\$/year] of rooftop farming options
CRF	Capital recovery factor for 15, 20, 30 years
$C^{im}$	Unit price of purchased electricity from the grid [\$/kWh]
$C^{ex}$	Tariff for electricity feed-back to grid [\$/kWh]
sales	Unit price of selling produced crop yield [\$/kg]
$\Psi$	Emission factor [kg/kWh]
$A_i$	Available roof area in $i$ site [m <sup>2</sup> ]

$Q^{h-dem}$ and $Q^{c-dem}$	Heating and cooling demand for each site
$E^{dem}$	Electricity demand for each site
$Q^{h-roof}$ and $Q^{c-roof}$	Thermal demand savings for each site
$Loss^{c-pipe}$ and $Loss^{h-pipe}$	Thermal loss rate for cooling ( $Lo^{c-pipe}$ ) and heating network ( $Lo^{h-pipe}$ )
$\bar{()}$	Upper bound value
$M$	The “big M” big enough values for $M_1$ and $M_2$

**Table A3 Definitions of variables**

<b>Variables</b>	<b>Definitions</b>
$TAC$	The objective of total annualised cost [\$/year]
$ACE$	The objective of annualised CO <sub>2</sub> emissions [ton/year]
<b>Binary Variables</b>	
$\varphi^{RF}$	=1 if select a certain crop and a certain planting pattern
$\beta^{CHP}$	=1 if CHP is on
$X^{CHP}$	=1 if CHP is switching from off to on
$\alpha^{cha}$	=1 if energy is charged into storage
$\alpha^{disc}$	=1 if energy is discharged from storage
$\delta^{ex}$	=1 if electricity is fed back to the grid
$\delta^{im}$	=1 if electricity is bought from the grid
$\delta^{DH}$	=1 if district heating network is built
$\delta^{DC}$	=1 if district cooling network is built
$\gamma^{DH}$	=1 if site $i$ receiving heating
$\gamma^{DC}$	=1 if site $i$ is receiving cooling
<b>Positive Variables</b>	
$CAPEX$	The capital cost of the whole system [\\$]
$FC$	The fuel cost [\$/year]
$MC$	The maintenance cost [\$/year]
$GC$	The grid electricity cost [\$/year]
$YI$	The food yield income [\$/year]
$CAP$	The installed capacity of each energy technology [kW]
$E^{CHP}$	The electricity output from CHP [kWh]
$Q^{HP}$	The heating output from heating pump [kWh]
$Q^B$	The heating output from boiler [kWh]
$Q^{A-CH}$	The cooling output from absorption chiller [kWh]
$Q^{E-CH}$	The cooling output from electric chiller [kWh]

$Q^{st}$	The cooling stored in storage tank [kWh]
$E^{E-CH}$	The electricity consumed by electric chiller [kWh]
$E^{st}$	The electricity stored in battery [kWh]
$E^{im}$	The electricity bought from the grid [kWh]
$E^{ex}$	The electricity sold back to the grid [kWh]
$Q^{hf(i,j)}$	The heating flow from site $i$ to $j$ [kWh]
$Q^{hf(j,i)}$	The heating flow from zone $j$ to $i$ [kWh]
$Q^{cf(i,j)}$	The cooling flow from site $i$ to $j$ [kWh]
$Q^{cf(j,i)}$	The cooling flow from site $j$ to $i$ [kWh]
$Q^{re}$	The heating output from CHP [kWh]
$Q^{cha}$	The cooling charge into cooling storage [kWh]
$Q^{disc}$	The cooling energy discharged [kWh]
$E^{cha}$	The electricity charge into battery storage [kWh]
$E^{disc}$	The electricity discharged [kWh]
$NG^B$	The natural gas consumed by boiler [kWh]
$NG^{CHP}$	The natural gas consumed by CHP [kWh]

---

The model is subject to the following constraints.

**Energy balances.** Three energy balances are modelled, i.e., electricity, cooling, and heating balances. Eq. (A1) constraints the electricity supply and demand balance.

$$E_{i,s,h}^{E-CH} + E_{i,s,h}^{ex} + E_{i,s,h}^{HP} + E_{i,s,h}^{cha} + E_{i,s,h}^{dem} = E_{i,s,h}^{disc} + E_{i,s,h}^{im} + E_{i,s,h}^{CHP} \quad (A1)$$

where  $E^{E-CH}$  is the electricity consumed by electric chiller,  $E^{ex}$  is electricity fed back to the grid,  $E^{HP}$  is electricity consumed by heat pump,  $E^{cha}$  is electricity charged into battery storage,  $E^{dem}$  is electrical demand to be met,  $E^{disc}$  is electricity discharged from battery storage,  $E^{im}$  is electricity purchased from the grid,  $E^{CHP}$  is the electricity generated by CHP.

Eq. (A2) constraints the heating supply and demand balance.

$$\begin{aligned} (Q_{i,s,h}^{h-dem} - \sum_v \sum_k \varphi_{i,v,k}^{RF} \times Q_{i,s,h,v,k}^{h-roof}) + \sum_j Q_{i,j,s,h}^{hf(i,j)} + Q_{i,s,h}^{A-CH} = \\ Q_{i,s,h}^{re} + Q_{i,s,h}^{HP} + Q_{i,s,h}^B + \sum_j Q_{j,i,s,h}^{hf(j,i)} \times (1 - Loss^{h-pipe}) \quad \forall j \neq i \end{aligned} \quad (A2)$$

where  $Q^{h-dem}$  is the representative heating demand,  $\varphi^{RF}$  is the binary variable to ensure only one rooftop farming option been selected,  $Q^{h-roof}$  is heating savings due to rooftop farming induced insulation improvement,  $Q^{hf(i,j)}$  is heating flow from site  $i$  to  $j$ ,  $Q^{A-CH}$  is heating been utilised to generate cooling by absorption chiller,  $Q^{re}$  is recovered heating from CHP power generation,  $Q^{HP}$  is heating supply from heat pump,  $Q^B$  is heating supply from boiler,  $Q^{hf(j,i)}$  is heating flow from site  $j$  to  $i$ ,  $Loss^{h-pipe}$  is heating loss rate during energy transfer.

Eq. (A3) constraints the cooling supply and demand balance.

$$\begin{aligned} (Q_{i,s,h}^{\text{c-dem}} - \sum_v \sum_k \phi_{i,v,k}^{\text{RF}} \times Q_{i,s,h,v,k}^{\text{c-roof}}) + Q_{i,s,h}^{\text{cha}} + \sum_j Q_{i,j,s,h}^{\text{cf}(i,j)} = \\ Q_{i,s,h}^{\text{A-CH}} + Q_{i,s,h}^{\text{E-CH}} + \sum_j Q_{j,i,s,h}^{\text{cf}(j,i)} \times (1 - \text{Loss}^{\text{c-pipe}}) + Q_{i,s,h}^{\text{disc}} \quad \forall j \neq i \end{aligned} \quad (\text{A3})$$

where  $Q^{\text{c-dem}}$  is the representative cooling demand,  $\phi^{\text{RF}}$  is the binary variable to ensure only one rooftop farming option been selected,  $Q^{\text{c-roof}}$  is cooling savings due to rooftop farming induced insulation improvement,  $Q^{\text{cha}}$  is cooling energy been charged into storage tank,  $Q^{\text{cf}(i,j)}$  is cooling flow from site  $i$  to  $j$ ,  $Q^{\text{A-CH}}$  is cooling supply from absorption chiller,  $Q^{\text{E-CH}}$  is cooling supply from electric chiller,  $Q^{\text{cf}(j,i)}$  is cooling flow from site  $j$  to  $i$ ,  $\text{Loss}^{\text{c-pipe}}$  is cooling loss rate during energy transfer,  $Q^{\text{disc}}$  is cooling been discharged from storage tank.

**Energy conversion.** The energy conversion constraints are shown by Eq. (A4).

$$\begin{aligned} Q_{i,s,h}^{\text{E-CH}} &= \eta^{\text{E-CH}} \times E_{i,s,h}^{\text{E-CH}} \\ Q_{i,s,h}^{\text{A-CH}} &= \eta^{\text{A-CH}} \times Q_{i,s,h}^{\text{A-CH}'} \\ Q_{i,s,h}^{\text{HP}} &= \eta^{\text{HP}} \times E_{i,s,h}^{\text{HP}} \\ Q_{i,s,h}^{\text{B}} &= \eta^{\text{B}} \times NG_{i,s,h}^{\text{B}} \\ E_{i,s,h}^{\text{CHP}} &= \eta^{\text{CHP}} \times NG_{i,s,h}^{\text{CHP}} \\ Q_{i,s,h}^{\text{re}} &= \text{H-to-P} \times E_{i,s,h}^{\text{CHP}} \end{aligned} \quad (\text{A4})$$

where  $\eta$  denotes efficiency,  $Q^{\text{E-CH}}$  is cooling supply from electric chiller,  $E^{\text{E-CH}}$  is the electricity consumed by electric chiller,  $Q^{\text{A-CH}}$  is cooling supply from absorption chiller,  $Q^{\text{A-CH}'}$  is heating been utilised to generate cooling by absorption chiller,  $Q^{\text{HP}}$  is heating supply from heat pump,  $E^{\text{HP}}$  is electricity consumed by heat pump,  $Q^{\text{B}}$  is heating supply from boiler,  $NG^{\text{B}}$  is natural gas been consumed by boiler,  $E^{\text{CHP}}$  is the electricity generated by CHP,  $NG^{\text{CHP}}$  is natural gas been consumed by CHP,  $Q^{\text{re}}$  is recovered heating from CHP power generation, H-to-P is the heat to power ratio for CHP.

**Operation constraints.** Operation constraints are implemented for CHP to avoid low demand operations and possible efficiency drop. The minimum part demand (MPL) as a percentage of full capacity is set to avoid CHP operating at low demand when the engine is on.

$$E_{i,s,h}^{\text{CHP}} \leq \beta_{i,s,h}^{\text{CHP}} \times M_1 \quad (\text{A5a})$$

$$E_{i,s,h}^{\text{CHP}} \geq (\beta_{i,s,h}^{\text{CHP}} - 1) \times M_2 + \text{MPL} \times \text{CAP}_i^{\text{CHP}} \quad (\text{A5b})$$

where  $\text{CAP}^{\text{CHP}}$  is CHP installed capacity, and  $\beta^{\text{CHP}}$  is a binary variable to control on/off status of CHP ( $\beta^{\text{CHP}} = 1$  is on).  $M_1$  and  $M_2$  are both big enough values.

To avoid frequently on/off of CHP, only switching on one time per day is allowed as formulated in Eq. (A6).

$$\sum_h \chi_{i,s,h}^{\text{CHP}} \leq 1 \quad (\text{A6a})$$

$$\chi_{i,s,h}^{\text{CHP}} \geq \beta_{i,s,h}^{\text{CHP}} - \beta_{i,s,h-1}^{\text{CHP}} \quad (\text{A6b})$$

$$\chi_{i,s,h}^{\text{CHP}} \leq 1 - \beta_{i,s,h-1}^{\text{CHP}} \quad (\text{A6c})$$

$$\chi_{i,s,h}^{\text{CHP}} \leq \beta_{i,s,h}^{\text{CHP}} \quad (\text{A6d})$$

where  $\chi$  is a binary variable to control the frequency of switching on/off.

To avoid drastic fluctuation of CHP's power output, the power output fluctuation between last and this time-step cannot be larger than a threshold (THR) of CHP's installed capacity.

$$E_{i,s,h}^{\text{CHP}} - E_{i,s,h-1}^{\text{CHP}} \leq \text{THR} \times \text{CAP}_i^{\text{CHP}} \quad (\text{A7a})$$

$$E_{i,s,h-1}^{\text{CHP}} - E_{i,s,h}^{\text{CHP}} \leq \text{THR} \times \text{CAP}_i^{\text{CHP}} \quad (\text{A7b})$$

where  $E^{\text{CHP}}$  is the electricity generated by CHP,  $\text{CAP}^{\text{CHP}}$  is the installed capacity of CHP.

**Storage constraints.** Battery and cooling storage are enabled in our model. Here, we show the battery storage constraints as illustrative example, the cooling storage constraints are similar from the modelling perspective with different inputs.

$$E_{i,s,h}^{\text{st}} = \eta^{\text{st}} \times E_{i,s,h-1}^{\text{st}} + \eta^{\text{cha}} \times E_{i,s,h}^{\text{cha}} - E_{i,s,h}^{\text{disc}} / \eta^{\text{disc}} \quad (\text{A8a})$$

$$E_{i,s,h}^{\text{st}} \leq \text{CAP}_i^{\text{st}} \quad (\text{A8b})$$

$$E_{i,s,h}^{\text{cha}} \leq \alpha_{i,s,h}^{\text{cha}} \times \overline{E_{i,s,h}^{\text{cha}}} \quad (\text{A8c})$$

$$E_{i,s,h}^{\text{disc}} \leq \alpha_{i,s,h}^{\text{disc}} \times \overline{E_{i,s,h}^{\text{disc}}} \quad (\text{A8d})$$

$$\alpha_{i,s,h}^{\text{disc}} + \alpha_{i,s,h}^{\text{cha}} \leq 1 \quad (\text{A8e})$$

where  $\eta^{\text{cha}}$ ,  $\eta^{\text{disc}}$ ,  $\eta^{\text{st}}$  are energy charge, discharge, and in-storage efficiency;  $\text{CAP}^{\text{st}}$  is the installed capacity of the battery;  $E^{\text{cha}}$  is electricity been charged into the battery;  $E^{\text{disc}}$  is electricity been discharged from the battery;  $E^{\text{st}}$  is electricity stored in battery;  $\alpha$  is a binary variable to avoid the cooling energy charging and discharging simultaneously.

**Grid connections.** The electricity purchased and fed-back to utility grid are formulated by Eq. (A9).

$$0 \leq E_{i,s,h}^{\text{ex}} \leq \delta_{i,s,h}^{\text{ex}} \times \overline{E_{i,s,h}^{\text{ex}}} \quad (\text{A9a})$$

$$0 \leq E_{i,s,h}^{\text{im}} \leq \delta_{i,s,h}^{\text{im}} \times \overline{E_{i,s,h}^{\text{im}}} \quad (\text{A9b})$$

$$\delta_{i,s,h}^{\text{ex}} + \delta_{i,s,h}^{\text{im}} \leq 1 \quad (\text{A9c})$$

where  $E^{\text{im}}$  and  $E^{\text{ex}}$  are electricity been purchased and fed-back to the grid;  $\delta^{\text{ex}}$  and  $\delta^{\text{im}}$  are binary variables to represent the export/import status and avoid power export and import simultaneously.

**Network constraints.** Cooling and heating network constraints are similar from the modelling perspective. The heating can only be transferred when two sites are connected via heating pipework as defined

in Eq. (A10a). The connection between two sites can only be done by at most one time in Eq. (A10b).

$$\sum_j Q_{i,j,s,h}^{\text{hf}(i,j)} \leq \delta_{i,j}^{\text{DH}} \times \overline{Q_{i,j,s,h}^{\text{hf}(i,j)}} \quad \forall j \neq i \quad (\text{A10a})$$

$$\delta_{i,j}^{\text{DH}} + \delta_{j,i}^{\text{DH}} \leq 1 \quad \forall j \neq i \quad (\text{A10b})$$

where  $Q^{\text{hf}(i,j)}$  is heating flow from site  $i$  to  $j$ ,  $\delta^{\text{DH}}$  is a binary variable to denote the connection or not among sites (1 is connected, 0 is not).

Similarly, cooling transfer can only happen if cooling pipework exists among sites as derived in Eq. (A11).

$$\sum_j Q_{i,j,s,h}^{\text{cf}(i,j)} \leq \delta_{i,j}^{\text{DC}} \times \overline{Q_{i,j,s,h}^{\text{cf}(i,j)}} \quad \forall j \neq i \quad (\text{A11a})$$

$$\delta_{i,j}^{\text{DC}} + \delta_{j,i}^{\text{DC}} \leq 1 \quad \forall j \neq i \quad (\text{A11b})$$

Each site  $i$  cannot simultaneously receive and transfer energy to other sites  $j$  as constrained by Eq. (A12).

$$\sum_j Q_{i,j,s,h}^{\text{cf}(i,j)} \leq \gamma_{i,s,h}^{\text{DC}} \times \overline{Q_{i,j,s,h}^{\text{cf}(i,j)}} \quad \forall j \neq i \quad (\text{A12a})$$

$$\sum_j Q_{j,i,s,h}^{\text{cf}(j,i)} \leq (1 - \gamma_{i,s,h}^{\text{DC}}) \times \overline{Q_{j,i,s,h}^{\text{cf}(j,i)}} \quad \forall j \neq i \quad (\text{A12b})$$

$$\sum_j Q_{i,j,s,h}^{\text{hf}(i,j)} \leq \gamma_{i,s,h}^{\text{DH}} \times \overline{Q_{i,j,s,h}^{\text{hf}(i,j)}} \quad \forall j \neq i \quad (\text{A12c})$$

$$\sum_j Q_{j,i,s,h}^{\text{hf}(j,i)} \leq (1 - \gamma_{i,s,h}^{\text{DH}}) \times \overline{Q_{j,i,s,h}^{\text{hf}(j,i)}} \quad \forall j \neq i \quad (\text{A12d})$$

where  $Q^{\text{cf}(i,j)}$  is cooling flow from site  $i$  to  $j$ ,  $Q^{\text{cf}(j,i)}$  is cooling flow from site  $j$  to  $i$ ,  $Q^{\text{hf}(i,j)}$  is heating flow from site  $i$  to  $j$ ,  $Q^{\text{hf}(j,i)}$  is heating flow from site  $j$  to  $i$ ,  $\gamma^{\text{DH}}$  and  $\gamma^{\text{DC}}$  are binary variables to control the status of transfer or receive for heating and cooling transfer.

## A.2 Parameterisation for case study

All the parameters in the case study are presented below.

**Table A4 A list of parameters applied in the optimisation model [6, 24, 44]**

Parameters	Definitions	Values
$C_{\text{CHP}}^{\text{CAP}}$	Unit capital cost of CHP [\$/kW]	800
$C_{\text{B}}^{\text{CAP}}$	Unit capital cost of boiler [\$/kW]	60
$C_{\text{E-CH}}^{\text{CAP}}$	Unit capital cost of electric chiller [\$/kW]	200
$C_{\text{A-CH}}^{\text{CAP}}$	Unit capital cost of absorption chiller [\$/kW]	250
$C_{\text{HP}}^{\text{CAP}}$	Unit capital cost of heat pump [\$/kW]	200
$C_{\text{pipe}}^{\text{CAP}}$	Unit capital cost of heating and cooling network [\$/m]	200
$C_{\text{b-st}}^{\text{CAP}}$	Unit capital cost of battery storage [\$/kWh]	700

$C_{c-st}^{CAP}$	Unit capital cost of cooling storage tank [\$/kWh]	60
$C_k^{CAP}$	Unit capital cost of k rooftop agriculture option [\$/m <sup>2</sup> ]	=12 when k=1, =45 when k=2~10
$DX_{i,j}$	Distance between zones	See Fig. 4b
$\eta^{CHP}$	Efficiency of CHP (ele)	0.4
H-to-P	Heat-to-power rate of CHP	0.8
$\eta^B$	Efficiency of boiler	0.85
$\eta^{E-CH}$	Efficiency of electric chiller	4
$\eta^{A-CH}$	Efficiency of absorption chiller	1.2
$\eta^{HP}$	Efficiency of heat pump	2.5
$\eta_{batt}^{st}$	Efficient of battery storage self-discharge	0.95
$\eta_{batt}^{cha/disc}$	Efficient of battery storage charge/discharge	0.93
$\eta_{cool}^{st}$	Efficient of cooling storage self-discharge	0.9
$\eta_{cool}^{cha/disc}$	Efficient of cooling storage charge/discharge	0.9
$C_h^{CHP-NG}$	Unit cost of natural gas for CHP [\$/kWh]	See Figure A1
$C_h^{B-NG}$	Unit cost of natural gas for boiler [\$/kWh]	See Figure A1
$C_{CHP}^{maint}$	Maintenance cost of CHP [\$/kWh]	0.003
$C_B^{maint}$	Maintenance cost of boiler [\$/kWh]	0.0003
$C_{E-CH}^{maint}$	Maintenance cost of electric chiller [\$/kWh]	0.001
$C_{A-CH}^{maint}$	Maintenance cost of absorption chiller [\$/kWh]	0.001
$C_{HP}^{maint}$	Maintenance cost of heat pump [\$/kWh]	0.001
$C_{b-st}^{maint}$	Maintenance cost of battery storage [\$/kWh]	0.003
$C_{c-st}^{maint}$	Maintenance cost of cooling storage tank [\$/kWh]	0.0003
CRF	Capital recovery factor for 15, 25, 30 years	0.103, 0.085, 0.073
$C_h^{im}$	Unit price of grid electricity purchasing at hour $h$ [\$/kWh]	See Figure A1
$C_h^{ex}$	Tariff for electricity sold back to grid at hour $h$ [\$/kWh]	See Figure A1
$E^{dem}$	Hourly electricity demand	See Figure 5
$\Psi_{grid}$	Emission factor of the grid electricity [kg/kWh]	0.45
$\Psi_{NG}$	Emission factor of natural gas power generation [kg/kWh]	0.18
$\psi_k^{agri}$	Emission factor of $k$ rooftop agriculture option	See Table 4
$A_i$	Available roof area in $i$ zones [m <sup>2</sup> ]	See Figure 4
$C_v^{RF}$	Unit price of selling each crop [US\$/kg]	See Table A12
MPL	Minimum part load of CHP	30%
M1	Big M for CHP model, the value may choose twice of peak electricity demand	see Figure 5
M2	Big M for CHP model, the value may choose twice of peak electricity demand	see Figure 5

$yield_{v,k}$	Annual yield [kg/ha/year]	See Table 3
$Q_{i,s,h}^{h-load}$	Hourly heating demand	See Figure 5
$Q_{i,s,h}^{c-load}$	Hourly cooling demand	See Figure 5
$Q_{i,s,h,k}^{h-roof}$	Heating demand saving rate by implementing rooftop farming options	4%, 6% of original demand
$Q_{i,s,h,k}^{c-roof}$	Cooling demand saving rate by implementing rooftop farming options	4%, 6% of original demand
THR	Threshold of CHP output variations as a percentage of its installed capacity	50%
Loss <sup>c-pipe</sup>	Cooling network thermal loss rate	6%
Loss <sup>h-pipe</sup>	Heating piping thermal loss rate	5%

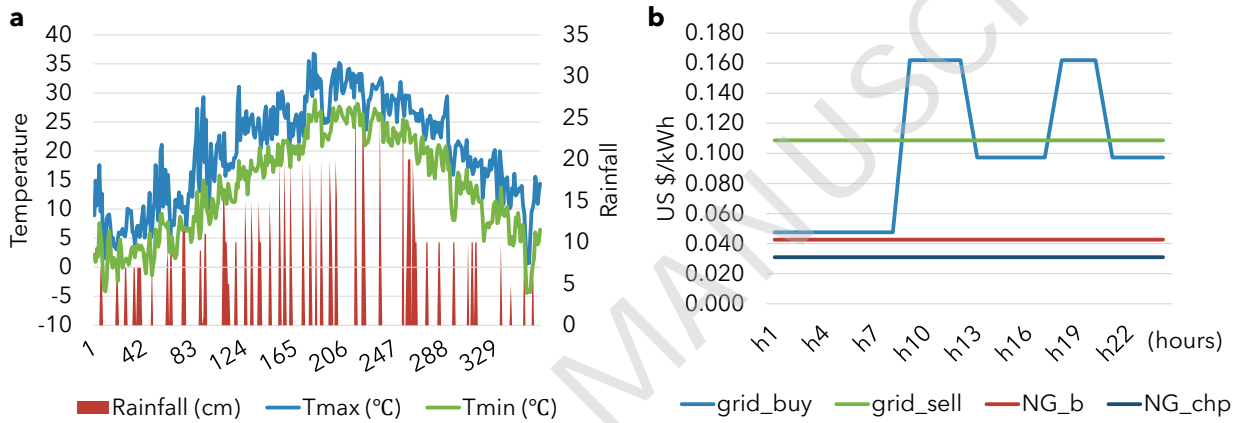


**Figure A1 Weather condition for DNDC simulation and energy prices in system optimisation model. a,** rainfall and temperature at daily basis; **b,** tariffs for purchased electricity (grid\_buy), fed-back to grid (grid\_sell), natural gas for CHP use (NG\_chp), and natural gas for boiler use (NG\_b).

**Table A5 Capital and operational costs for the simulated lettuce**

lettuce	OPT1	OPT2	OPT3	OPT4	OPT5	OPT6	OPT7	OPT8	OPT9	OPT10
Capital cost (\$/ha)	120,000	450,000	450,000	450,000	450,000	450,000	450,000	450,000	450,000	450,000
Fertiliser (\$/ha/year)	43,200	35,760	35,760	35,760	35,760	35,760	35,760	35,760	35,760	35,760
Water (\$/ha/year)	357	1,486	1,377	1,324	1,328	1,311	1,235	1,329	1,302	1,266
Energy (\$/ha/year)	945	9,450	9,450	9,450	11,840	11,840	11,840	15,130	15,130	15,130
Labor (\$/ha/year)	63,428	105,714	105,714	105,714	105,714	105,714	105,714	105,714	105,714	105,714

**Table A6 Capital and operational costs for the simulated broccoli**

broccoli	OPT1	OPT2	OPT3	OPT4	OPT5	OPT6	OPT7	OPT8	OPT9	OPT10
Capital cost (\$/ha)	120,000	450,000	450,000	450,000	450,000	450,000	450,000	450,000	450,000	450,000
Fertiliser (\$/ha/year)	14,400	14,400	14,400	14,400	14,400	14,400	14,400	14,400	14,400	14,400
Water (\$/ha/year)	357	1,006	1,004	987	1,019	1,024	1,028	1,106	1,026	1,032
Energy (\$/ha/year)	945	9,450	9,450	9,450	11,840	11,840	11,840	15,130	15,130	15,130
Labor (\$/ha/year)	63,428	105,714	105,714	105,714	105,714	105,714	105,714	105,714	105,714	105,714

**Table A7 Capital and operational costs for the simulated tomato**

tomato	OPT1	OPT2	OPT3	OPT4	OPT5	OPT6	OPT7	OPT8	OPT9	OPT10
Capital cost (\$/ha)	120,000	450,000	450,000	450,000	450,000	450,000	450,000	450,000	450,000	450,000
Fertiliser (\$/ha/year)	29,714	10,588	10,588	10,588	10,588	10,588	10,588	10,588	10,588	10,588
Water (\$/ha/year)	1,429	6,064	5,483	4,981	5,192	4,763	4,387	4,974	4,384	3,841
Energy (\$/ha/year)	945	9,450	9,450	9,450	11,840	11,840	11,840	15,130	15,130	15,130

Labor (\$/ha/year)	63,428	105,714	105,714	105,714	105,714	105,714	105,714	105,714	105,714	105,714
--------------------	--------	---------	---------	---------	---------	---------	---------	---------	---------	---------

**Table A8 Capital and operational costs for the simulated cabbage**

cabbage	OPT1	OPT2	OPT3	OPT4	OPT5	OPT6	OPT7	OPT8	OPT9	OPT10
Capital cost (\$/ha)	120,000	450,000	450,000	450,000	450,000	450,000	450,000	450,000	450,000	450,000
Fertiliser (\$/ha/year)	106,285	106,285	106,285	106,285	106,285	106,285	106,285	106,285	106,285	106,285
Water (\$/ha/year)	1,000	2,399	2,154	2,056	1,736	1,421	1,243	1,564	1,336	1,207
Energy (\$/ha/year)	945	9,450	9,450	9,450	11,840	11,840	11,840	15,130	15,130	15,130
Labor (\$/ha/year)	63,428	105,714	105,714	105,714	105,714	105,714	105,714	105,714	105,714	105,714

**Table A9 Capital and operational costs for the simulated potato**

potato	OPT1	OPT2	OPT3	OPT4	OPT5	OPT6	OPT7	OPT8	OPT9	OPT10
Capital cost (\$/ha)	120,000	450,000	450,000	450,000	450,000	450,000	450,000	450,000	450,000	450,000
Fertiliser (\$/ha/year)	121,714	162,285	162,285	162,285	162,285	162,285	162,285	162,285	162,285	162,285
Water (\$/ha/year)	214	896	884	865	1,205	997	911	1,434	1,306	1,197
Energy (\$/ha/year)	945	9,450	9,450	9,450	11,840	11,840	11,840	15,130	15,130	15,130
Labor (\$/ha/year)	63,428	105,714	105,714	105,714	105,714	105,714	105,714	105,714	105,714	105,714

**Table A10 Capital and operational costs for the simulated radish**

radish	OPT1	OPT2	OPT3	OPT4	OPT5	OPT6	OPT7	OPT8	OPT9	OPT10
Capital cost (\$/ha)	120,000	450,000	450,000	450,000	450,000	450,000	450,000	450,000	450,000	450,000
Fertiliser (\$/ha/year)	12,580	15,725	15,725	15,725	15,725	15,725	15,725	15,725	15,725	15,725

Water (\$/ha/year)	214	843	734	641	997	931	656	986	909	721
Energy (\$/ha/year)	945	9,450	9,450	9,450	11,840	11,840	11,840	15,130	15,130	15,130
Labor (\$/ha/year)	63,428	105,714	105,714	105,714	105,714	105,714	105,714	105,714	105,714	105,714

**Table A11 Capital and operational costs for the simulated celery**

celery	OPT1	OPT2	OPT3	OPT4	OPT5	OPT6	OPT7	OPT8	OPT9	OPT10
Capital cost (\$/ha)	120,000	450,000	450,000	450,000	450,000	450,000	450,000	450,000	450,000	450,000
Fertiliser (\$/ha/year)	61,714	68,114	68,114	68,114	68,114	68,114	68,114	68,114	68,114	68,114
Water (\$/ha/year)	357	2,602	2,460	2,379	2,091	1,980	1,874	3,197	3,001	2,836
Energy (\$/ha/year)	945	9,450	9,450	9,450	11,840	11,840	11,840	15,130	15,130	15,130
Labor (\$/ha/year)	63,428	105,714	105,714	105,714	105,714	105,714	105,714	105,714	105,714	105,714

**Table A12 Unit price for selling each crop**

Crop	lettuce	broccoli	tomato	cabbage	potato	radish	celery
Unit price [US\$/kg]	0.62	0.90	0.50	0.30	0.32	0.32	0.78